Med

Article

Lymphocyte alterations and elevated complement signaling are key features of refractory myasthenia gravis

Graphical abstract

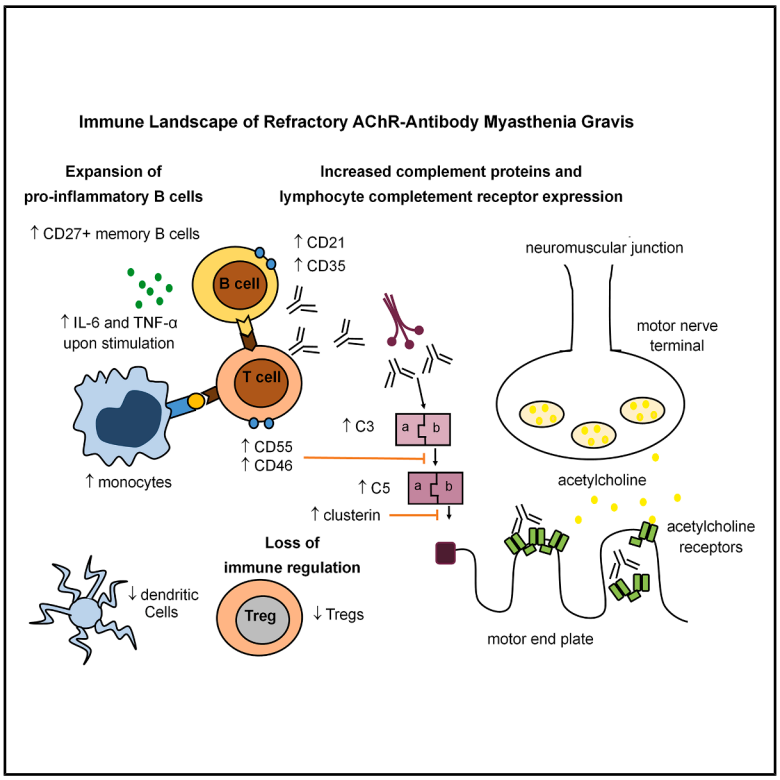

Highlights

- Patients with refractory myasthenia gravis exhibit a distinct immune signature
- Increased memory and pro-inflammatory B cells and reduced Tregs and DCs
- Elevated complement protein levels and receptor expression on lymphocytes
- Low baseline B cell frequency associates with poor clinical response to rituximab

Authors

Katherine C. Dodd, Kirsten Baillie, James K.L. Holt, ..., Wioleta M. Zelek, Jon Sussman, Madhvi Menon

Correspondence

katherine.dodd@manchester.ac.uk (K.C.D.), madhvi.menon@manchester.ac.uk (M.M.)

In brief

Dodd et al. report an immune imbalance in refractory myasthenia gravis, characterized by expanded memory and pro-inflammatory B cells, elevated complement proteins, and reduced Tregs. Low baseline B cell counts predict poor response to rituximab, with persistent plasmablasts, thus highlighting biomarkers and potential therapeutic strategies targeting plasma cells, complement, and Tregs.

Translation to Patients

Dodd et al., 2026, Med 7, 100987
March 13, 2026
https://doi.org/10.1016/j.medj.2025.100987

CellPress

Please cite this article in press as: Dodd et al., Lymphocyte alterations and elevated complement signaling are key features of refractory myasthenia gravis, Med (2025), https://doi.org/10.1016/j.medj.2025.100987

Med

CellPress
OPEN ACCESS

Article

Lymphocyte alterations and elevated complement signaling are key features of refractory myasthenia gravis

Katherine C. Dodd,[1,2,*] Kirsten Baillie,[3] James K.L. Holt,[4] M. Isabel Leite,[5,6] Lijing Lin,[7] Peter W. West,[1] James A.L. Miller,[8] Jennifer Spillane,[9] Stuart Viegas,[10] Wioleta M. Zelek,[3] Jon Sussman,[2] and Madhvi Menon[1,11,*]

[1]The Lydia Becker Institute for Immunology and Inflammation, University of Manchester, Manchester M13 9NT, UK
[2]Manchester Centre for Clinical Neurosciences, the Northern Care Alliance NHS Foundation Trust, Salford M6 8HD, UK
[3]UK Dementia Research Institute Cardiff and Division of Infection and Immunity, School of Medicine, Cardiff University, Cardiff, Wales CF14 4XN, UK
[4]The Walton Centre NHS Foundation Trust, Liverpool L9 7LJ, UK
[5]The University of Oxford, Oxford OX1 4BH, UK
[6]Oxford University Hospitals NHS Foundation Trust, Oxford OX3 9DU, UK
[7]Division of Informatics, Imaging and Data Sciences, University of Manchester, Manchester M13 9NT, UK
[8]Newcastle Hospitals NHS Foundation Trust, Newcastle NE1 4LP, UK
[9]University College London Hospitals NHS Foundation Trust, London WC1N 3BG, UK
[10]Imperial College Healthcare NHS Trust, London W2 1NY, UK
[11]Lead contact
*Correspondence: katherine.dodd@manchester.ac.uk (K.C.D.), madhvi.menon@manchester.ac.uk (M.M.)
https://doi.org/10.1016/j.medj.2025.100987

CONTEXT AND SIGNIFICANCE Myasthenia gravis (MG) is an autoimmune disorder in which antibodies disrupt communication between nerves and muscles, causing weakness. This study compared patients with refractory MG, who respond poorly to standard therapies, with treatment-responsive or treatment-naive patients and healthy controls. Refractory patients exhibited a distinct immune signature characterized by expanded memory B cells, elevated complement proteins, reduced regulatory T cells, and increased pro-inflammatory cytokines (interleukin [IL]-6 and tumor necrosis factor alpha [TNF-α]). Individuals with very low baseline B cell counts responded poorly to rituximab and frequently retained antibody-producing plasmablasts. These findings identify potential biomarkers of treatment resistance and highlight promising therapeutic targets involving plasma cells, complement, and immune regulation.

SUMMARY

Background: A significant proportion of patients with myasthenia gravis (MG) remain refractory to standard immunosuppressive therapy, and biomarkers to help guide treatment decisions are lacking. We investigated whether refractory disease is associated with a distinct circulating immune profile.

Methods: We performed comprehensive immune phenotyping of peripheral blood from patients with acetylcholine-receptor-antibody-positive MG with differing treatment requirements and compared them with healthy controls. In a subset of refractory patients treated with anti-CD20 therapy, B cell reconstitution and clinical response were evaluated.

Findings: Refractory MG patients displayed the highest frequency of memory B cells and increased production of interleukin (IL)-6 and tumor necrosis factor alpha (TNF-α) upon Toll-like receptor/CD40 activation *in vitro*. These changes were accompanied by a dramatic loss of regulatory T cells (Tregs) and dendritic cells. Refractory MG was further characterized by elevated circulating complement proteins (C3, C5, and clusterin) and increased expression of complement receptors on lymphocytes. Following anti-CD20 therapy, residual plasmablasts persisted in circulation. Notably, a low baseline B cell frequency (<3%) was associated with poor clinical response to rituximab in refractory disease, although the sample size was limited.

Please cite this article in press as: Dodd et al., Lymphocyte alterations and elevated complement signaling are key features of refractory myasthenia gravis, Med (2025), https://doi.org/10.1016/j.medj.2025.100987

Conclusions: Our findings define a distinct immune signature in refractory MG, identify potential biomarkers of treatment resistance, and highlight plasma cell depletion, IL-6 or complement inhibition, and Treg expansion as promising therapeutic avenues.

Funding: Funding was received from the NorthCare Charity, Myaware, the Academy of Medical Sciences, and the Neuromuscular Study Group.

INTRODUCTION

In myasthenia gravis (MG), autoantibodies target the neuromuscular junction, causing fatigable muscle weakness around the eyes (ocular) and often the bulbar, respiratory, and limb muscles (generalized). MG is a highly heterogeneous disease of variable severity, with many refractory to standard immunosuppression, with resultant implications upon quality of life and large healthcare resource utilization.[1,2]

Around 85% of cases are due to antibodies targeting the acetylcholine receptor (AChR-abs).[3] AChR-MG can be divided into three main subgroups: (1) early-onset MG (EOMG), usually in females in their 20s–30s with thymic lymphoid follicular hyperplasia; (2) late-onset MG (LOMG), usually in males in their 60s–70s; and (3) thymoma-related MG. Generalized MG is initially treated with the acetylcholinesterase inhibitor pyridostigmine, followed by corticosteroids and, if necessary, steroid-sparing immunosuppressants. B cell-depleting agents have historically been reserved for refractory disease. Emerging therapies, including complement, neonatal Fc receptor (FcRn), or interleukin (IL)-6 inhibitors, show promise,[4] but patient selection is unclear.

There is a lack of reliable biomarkers to individualize treatment, and the pathophysiology of treatment resistance is poorly understood. AChR-ab titers do not correlate with disease severity, though the rate of change has been linked to outcome.[5,6] Clinical predictors of disease severity include thymoma, being overweight, and female gender.[7,8] MG is T cell dependent,[9] with functional impairments in regulatory T cells (Tregs) previously reported.[10,11] Alterations in B cell populations have also been described, including an expansion of class-switched memory B cells, circulating plasmablasts, and plasma cells.[12–14] Immunosuppression reduces naive B cells and increases naive T cells[12,15]; however, biomarkers indicative of an effective dose remain unknown. Previous immunophenotyping studies in MG have largely compared unstratified patient cohorts to healthy controls.

The innate immune system is increasingly recognized as contributing to autoimmune disease pathology. Myeloid cells, including dendritic cells (DCs) and monocytes, are recognized to contribute to the initiation, perpetuation, and end-organ damage in MG.[16–18] Disruptions in DC and monocyte phenotypes have recently been implicated in MG pathophysiology[14,19,20]; however, circulating myeloid cell frequencies remain poorly characterized.

AChR-abs activate the complement system, leading to membrane attack complex deposition at the neuromuscular junction.[21] Circulating complement findings in MG are inconsistent: some studies have reported lower circulating C3 and C4 levels,[22,23] whereas others have reported unchanged or elevated levels of C3, C3b, and C5a.[24,25] Complement also modulates lymphocyte function, with C3- or C4-deficient experimental autoimmune MG (EAMG) mice exhibiting increased B cell apoptosis.[26] Complement receptor 2 (cluster of differentiation [CD]21) binds to C3d and promotes B cell survival, activation, and antibody production.[27,28] It has been found to be upregulated on AChR-ab-producing B cells and correlated with AChR immunoglobulin (Ig)G titers.[29] In contrast, B cell complement receptor 1 (CD35), which binds to C3b/C4b and promotes regulatory B cell function, is downregulated on B cells in other autoimmune conditions.[30,31]

Complement regulators CD55 (decay-accelerating factor), CD59 (protectin), and CD46 (membrane cofactor protein) provide negative feedback to complement activation and are expressed by T cells. EAMG mice lacking CD55 and/or CD59 are more susceptible to disease and display a profoundly severe phenotype.[32,33] CD55, CD59, and CD46 also modulate T cell function[34,35]; however, their expression on T cells in MG has not been previously characterized.

In the era of emerging high-cost targeted therapies for MG, identifying biomarkers that predict treatment resistance is of increasing clinical importance. Here, we undertook an observational cohort analysis to define immune cell profiles in refractory MG, with the aim of informing personalized therapeutic strategies and uncovering novel targets for intervention.

RESULTS

Clinical cohorts

The study recruited 61 participants with AChR-MG and 21 controls, without autoimmune disease or cancer (solid organ or hematological). Participants with AChR-MG were stratified into four cohorts to distinguish between effects of disease severity and treatment: stable non-immunosuppressed (SNIS; stable on only low-dose acetylcholinesterase inhibitors [$\leq$120 mg/day] for >2 years), stable immunosuppressed (SIS; stable for >2 years on azathioprine or mycophenolate mofetil with $\leq$5 mg/day prednisolone), refractory (eligible for rituximab under NHS England criteria[36]; on corticosteroids and other immunosuppression with ongoing disease activity or explosive bulbar onset), and treatment naive (TN; diagnosed within the previous 6 months, with no immunosuppression).

All participants with MG were AChR-ab positive at diagnosis; those with thymoma were excluded. The patient groups were compared to age- and gender-matched controls. Four participants were excluded (due to subsequent diagnosis of chronic myeloid leukemia [n = 1], thymoma [n = 1], high c-reactive protein (CRP) and suspicion of concurrent infection [n = 1], or a grossly abnormal immune phenotype of uncertain cause [n = 1]). The final cohort comprised 58 participants with AChR-MG (n = 17

Please cite this article in press as: Dodd et al., Lymphocyte alterations and elevated complement signaling are key features of refractory myasthenia gravis, Med (2025), https://doi.org/10.1016/j.medj.2025.100987

CellPress
OPEN ACCESS

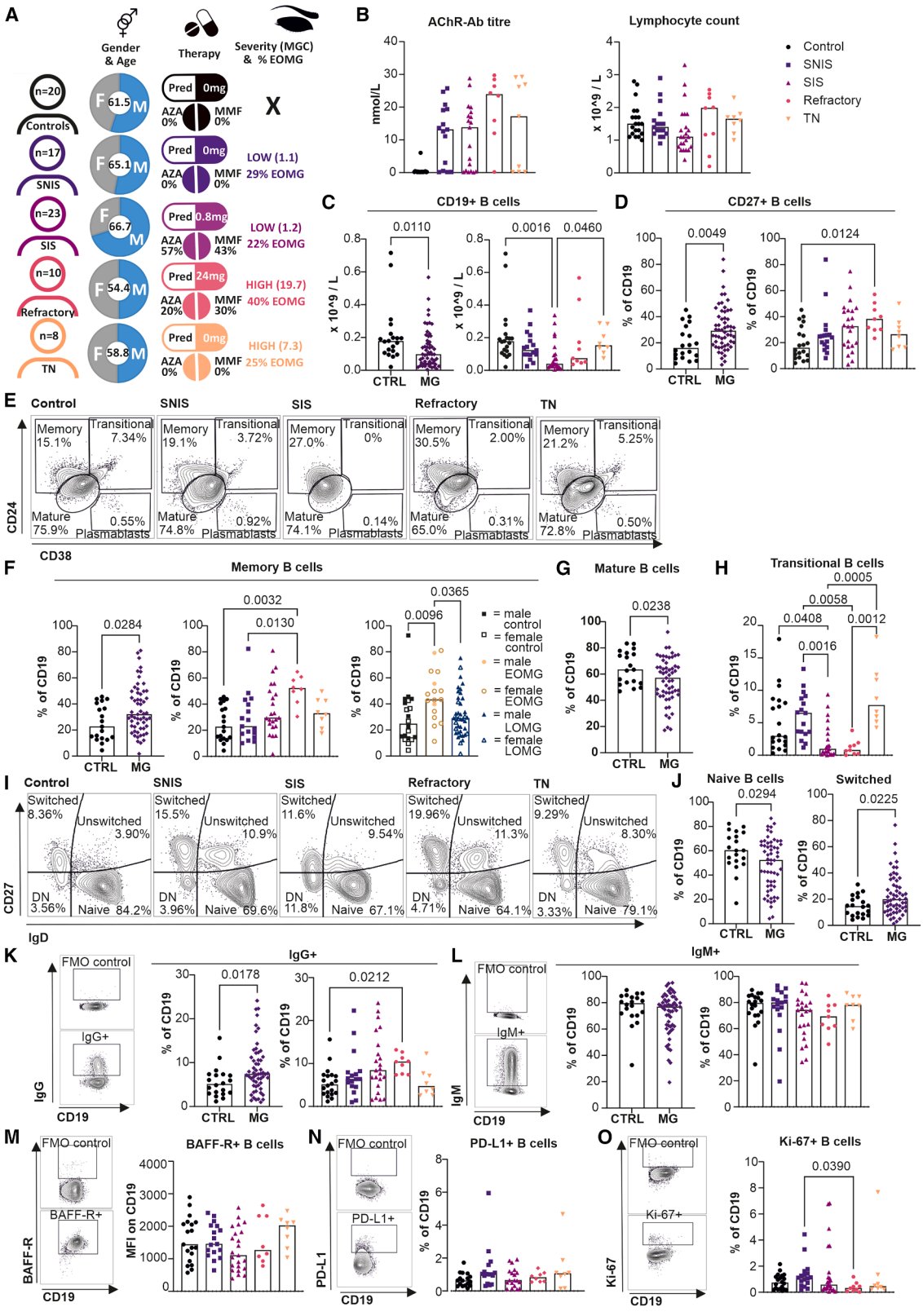

(legend on next page)

Please cite this article in press as: Dodd et al., Lymphocyte alterations and elevated complement signaling are key features of refractory myasthenia gravis, Med (2025), https://doi.org/10.1016/j.medj.2025.100987

SNIS, $n = 23$ SIS, $n = 10$ refractory, and $n = 8$ TN) and 20 controls. Table S1 and Figure 1A show the demographics and clinical features of the included participants.

Expansion of memory B cells in refractory MG

To determine whether B cell frequency reflects effective immunosuppression better than total lymphocyte count, peripheral blood mononuclear cells (PBMCs) were analyzed by flow cytometry. The AChR titer and total lymphocyte count did not differ between disease cohorts, and the antibody titer did not correlate with disease severity (Figures 1B and S1A). We observed a significant reduction in CD19 count in MG compared to controls, primarily in the SIS cohort, but this did not distinguish between those on effective immunosuppression (SIS) and those who were refractory (Figures 1C, gating strategy, and S1B). There was no difference in PBMC count between the cohorts (Figure S1C).

Further analysis revealed that $CD27^+$ B cells were significantly expanded in MG, with the greatest increase in the refractory cohort when comparing disease subgroups (Figures 1D, S1D, and S1E). Next, we evaluated the expression of CD38 and CD24 in B cells and found that memory B cells were expanded in patients, again significantly in the refractory cohort (Figures 1E and 1F). When the patient cohort was grouped by age of disease onset, we observed an expansion of memory B cells and $CD27^+$ B cells in those with EOMG compared to LOMG, independent of gender or age (Figures 1F, S1E, and S1F). Memory B cell frequency showed a weak positive correlation with disease severity (Figure S1G).

Furthermore, we observed a reduction in mature B cell frequency in patients with MG compared to controls (Figure 1G), with no differences between MG subgroups (Figure S1H). Both immunosuppressed groups (SIS and refractory) displayed a reduction in transitional B cell frequency (Figure 1H), a known consequence of azathioprine and mycophenolate,[37] with no overall difference between patients and controls (Figure S1I). There were no differences observed in the frequency of circulating plasmablasts, when measured as $CD38^{++}CD24^-$, $CD38^{++}CD27^{++}$, or Blimp-1^+, between cohorts (Figures S1J–S1L).

We next characterized B cells into naive, class-switched memory, unswitched memory, and double-negative memory B cell subsets based on IgD and CD27 expression (Figure 1I). Patients with MG showed an expansion of class-switched memory B cells, accompanied by reduced naive B cells, compared to controls (Figures 1J, S1M, and S1N), with no significant differences in subset frequencies between EOMG and LOMG (Figure S1N). IgG expression was increased in patients with MG compared to controls (Figure 1K), with no differences in IgM expression (Figure 1L). Frequencies of unswitched and double-negative memory B cells were comparable between patients and controls (Figures S1O and S1P).

We examined the expression of B cell activating factor-receptor (BAFF-R) and programmed death-ligand 1 (PD-L1) on B cells and did not observe any differences in relation to disease activity or treatment (Figures 1M, 1N, S1Q, and S1R). Ki-67 expression (indicative of proliferation) was reduced in refractory MG compared to SNIS, but no significant differences were observed between other cohorts (Figures 1O and S1R). This may be due to functional exhaustion of B cells in refractory disease or may reflect the more extensive immunosuppressive therapies used in refractory patients.

B cells display a pro-inflammatory phenotype in refractory MG

Next, we stimulated PBMCs from patients with MG and controls for 48 h with CD40L, CpG-B (Toll-like receptor [TLR]9 agonist), or R848 (TLR7 agonist) and assessed cytokine production. Interestingly, patients with MG produced significantly more pro-inflammatory cytokine IL-6 upon activation via TLR9, TLR7, or CD40 (compared to controls), and this was highest in those with refractory disease upon CD40 activation (Figure 2A). Tumor necrosis factor alpha (TNF-α) production was significantly increased in patients with MG upon activation via TLR9 and TLR7 but not CD40 (Figure 2B). When comparing disease subgroups, TNF-α production upon TLR9 activation was highest in the refractory cohort (Figure 2B). IL-10 production was increased in patients with MG only upon TLR9 activation, with no differences observed between patient subgroups (Figure 2C). No differences were observed between those with EOMG and LOMG (Figures 2A–2C).

Figure 1. B cell alterations in patients with AChR-MG

(A) Infographic showing clinical characteristics, demographics, and treatment of cohorts.

(B) AChR titer in the control ($n = 19$), SNIS ($n = 15$), SIS ($n = 19$), refractory ($n = 8$), and TN ($n = 9$) cohorts and total lymphocyte count in the control ($n = 20$) SNIS ($n = 17$), SIS ($n = 22$), refractory ($n = 8$), and TN ($n = 8$) cohorts.

(C and D) CD19 count in analysis of PBMCs (C) and $CD27^+$ frequency within $CD19^+$ B cells (D) in control ($n = 20$) compared to MG ($n = 57$) and between the control ($n = 20$), SNIS ($n = 17$), SIS ($n = 22$), refractory ($n = 9$), and TN ($n = 8$) subgroups.

(E) Representative fluorescence-activated cell sorting (FACS) plots for CD24 vs. CD38, gated on $CD19^+$ live lymphocytes, for control, SNIS, SIS, refractory, and TN cohorts.

(F) Memory B cell frequency within $CD19^+$ B cells in control ($n = 20$) compared to MG ($n = 57$); between control ($n = 20$), SNIS ($n = 17$), SIS ($n = 22$), refractory ($n = 9$), and TN ($n = 8$) subgroups; and between EOMG ($n = 17$) and LOMG ($n = 40$).

(G) Mature B cell frequency within $CD19^+$ B cells in control ($n = 20$) compared to MG ($n = 57$).

(H) Transitional B cell frequency within $CD19^+$ B cells in control ($n = 20$), SNIS ($n = 17$), SIS ($n = 22$), refractory ($n = 9$), and TN ($n = 8$) subgroups.

(I) Representative FACS plots displaying CD27 and IgD expression on B cells, gated on $CD19^+$ live lymphocytes, for control, SNIS, SIS, refractory, and TN cohorts.

(J) Switched and naive (IgD^+CD27^-) B cell frequency within $CD19^+$ B cells in control ($n = 20$) compared to MG ($n = 57$).

(K and L) IgG^+ (K) and IgM^+ (L) B cell gating and frequency between control ($n = 20$) and MG ($n = 57$) and between control ($n = 20$), SNIS ($n = 17$), SIS ($n = 22$), refractory ($n = 9$), and TN ($n = 8$) subgroups.

(M–O) BAFF-R gating strategy and mean fluorescent intensity on B cells (M) and PD-$L1^+$ (N) and Ki-67^+ (O) gating and B cell frequency in control ($n = 20$), SNIS ($n = 17$), SIS ($n = 22$), refractory ($n = 9$), and TN ($n = 8$) subgroups.

Flow cytometry was performed on PBMCs. Graphs show individual participant data, with bars representing the median values.

Please cite this article in press as: Dodd et al., Lymphocyte alterations and elevated complement signaling are key features of refractory myasthenia gravis, Med (2025), https://doi.org/10.1016/j.medj.2025.100987

CellPress
OPEN ACCESS

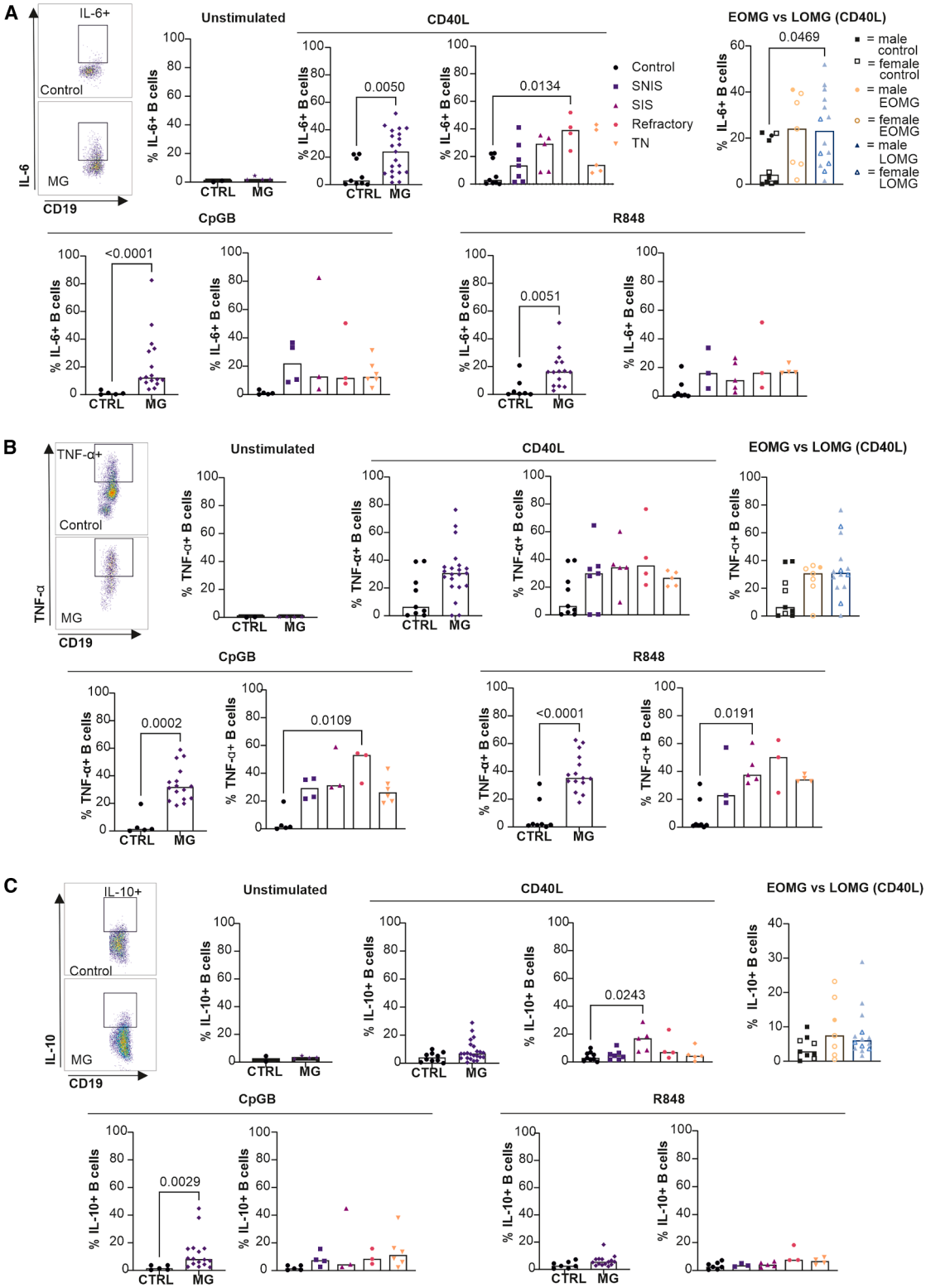

(legend on next page)

Please cite this article in press as: Dodd et al., Lymphocyte alterations and elevated complement signaling are key features of refractory myasthenia gravis, Med (2025), https://doi.org/10.1016/j.medj.2025.100987

Reduced frequencies of Tregs and DCs in refractory MG

To determine if these B cell changes, or the disease phenotype, may relate to changes in the T cell compartment, the T cell profile was analyzed. CD3 count did not differ between groups (Figure 3A), but CD4 frequency was higher in patients with MG compared to controls, mainly in those on immunosuppression (Figures 3B, S2A, and S2B). $CD8^+$ T cell frequencies did not significantly differ (Figure S2C), but the number of $CD4^+CD8^+$ double-positive T cells was lower in MG, particularly in the SIS cohort (Figure S2D).

Analysis of $CD4^+$ T cell subsets revealed an expansion of naive T cells in refractory MG (Figures 3C, S2E, and S2F). Effector memory T cells were reduced in both immunosuppressed groups (SIS and refractory), whereas central memory and terminally differentiated (TD) effector cell frequencies did not significantly differ between subgroups (Figures 3C, S2E, and S2F). Notably, $CD4^+CD25^+FoxP3^+$ Tregs were significantly reduced in the refractory cohort compared to controls and SNIS patients (Figures 3D–3F). Treg frequencies negatively correlated with disease severity and disease-related quality-of-life scores (Figure 3G), suggesting a potential role in ameliorating disease. No significant difference in CD8 Tregs was seen (Figure S2G). As Tregs are known to suppress pro-inflammatory B cells, we next examined whether the loss of Tregs was associated with the expansion of effector B cells. Indeed, we observed a significant negative correlation between IL-6-producing B cells and Treg frequencies (Figure 3H). No differences in Tregs were observed between EOMG and LOMG (Figure S2H). In contrast to previous reports of expanded circulating T follicular helper (Tfh) cell frequencies in MG,[38,39] we observed a trend toward reduction in patients with MG, particularly in the refractory cohort (Figures 3I and S2I).

Further, we examined the expression of the immune checkpoint molecules programmed cell death protein-1 (PD-1) and cytotoxic T lymphocyte antigen 4 (CTLA-4), given that blockade of these pathways can induce MG-like syndromes and that genetic studies have linked CTLA-4 variants to MG.[40–43] PD-1 and CTLA-4 expression by $CD4^+$ and $CD8^+$ T cells, as well as Tregs, did not significantly differ between MG cohorts and controls (Figures 3J, S2J, and S2K).

Myeloid compartment changes seen in refractory MG

Given the interplay between the adaptive and innate immune systems, we next investigated whether alterations in myeloid cells might contribute to reduced Treg frequencies in refractory MG (gating strategy in Figure S3A). Although there were no differences in DC frequencies between all patients with MG and controls, there was a dramatic reduction in the refractory MG cohort when comparing disease subgroups (Figure 4A). Both plasmacytoid DC (pDC) and myeloid DC (mDC) frequencies were decreased in the refractory cohort (Figures 4B and S3B); however, the pDC:mDC ratios were similar between patient groups (Figure S3C). Treg frequency does not correlate with DC frequency but does show a weak correlation with pDC frequency (Figure 4C). Of note, pDCs showed greater correlation with disease severity and quality-of-life scores than total DC frequency (Figure 4C). Monocytes were expanded across MG cohorts (apart from SNIS) and skewed toward the classical phenotype (Figures 4D, 4E, and S3D). Natural killer (NK) cell frequencies and subsets did not show any significant differences between patients with MG and controls or between patient cohorts (Figures 4F, 4G, S3E, and S3F). The SIS group exhibited reduced frequencies of $CD86^+$ monocytes and DCs, whereas no differences were observed in CD86 expression in NK cells and CD80 expression across all myeloid subsets (Figures S3G–S3I).

Complement receptor expression on lymphocytes and circulating complement proteins is elevated in refractory MG

Given that AChR-abs activate the complement system,[44] we examined circulating complement proteins (proteins TCC, Ba, C1q, C4, C9, CR1, FH, FHR4, FI, iC3b, properdin, and FHR125) in MG and their association with disease and treatment. Although there were no differences observed when comparing all patients with MG to controls (Figure S4A) or between EOMG and LOMG (Figure S4B), the circulating levels of C3, C5, and clusterin were significantly elevated in refractory disease when comparing patient subgroups (Figures 5A, 5B, and S4C). Further, C3, C5, and clusterin levels positively correlated with disease severity and quality-of-life scores (Figures 5B and S4D).

Complement is known to cause disruption at the neuromuscular junction[26]; however, its interaction with lymphocytes remains unclear. To explore this, we examined CD21 and CD35 expression in B cells and discovered increased mean fluorescence intensity of both receptors in patients with MG compared to controls (Figure 5C). However, frequencies of CD35-expressing B cells, but not CD21-expressing B cells, were reduced in patients with MG compared to controls, with no differences between patient subgroups (Figure S4E).

We next examined the expression of complement receptors CD55, CD46, and CD59 on T cells (Figures S4F and S4G). The intensity of expression of CD55 and CD46, but not CD59, was significantly higher in CD4 and CD8 T cells (Figure 5D). When examined by treatment subgroups, CD55 expression was highest in the refractory cohort in CD8 T cells and in both refractory and SIS cohorts in CD4 T cells (Figures 5E, 5F, and S4I); however, there was no significant difference in the intensity of CD46 expression between subgroups (Figure S4H). Frequencies of $CD55^+$ CD4/CD8 T cells and $CD46^+$ CD4 T cells were significantly expanded in MG, with $CD55^+$ and $CD46^+$ CD8 T cell frequencies highest in the refractory cohort (Figures 5F and S4J), indicating ongoing complement-mediated pathology in refractory disease. No differences were observed in CD59-expressing T cells.

Further, we stimulated lymphocytes with R848, anti-CD3, and anti-CD28 while inhibiting the complement receptors CD21,

Figure 2. B cell cytokine production in patients with AChR-MG

Representative FACS plot demonstrating IL-6^+ (A), TNF-α^+ (B), and IL-10^+ (C) B cells in control compared to MG and IL-6^+, TNF-α^+, and IL-10^+ B cell frequency when unstimulated and following stimulation with CD40L, CpG-B, and R848 in control (n = 5 CpG-B, n = 7 R848, and n = 10 CD40L) compared to MG (n = 16 CpG-B, n = 15 R848, and n = 23 CD40L) and when split into early-onset (n = 7) or late-onset (n = 15) MG. Flow cytometry was performed on peripheral blood mononuclear cells (PBMCs). Graphs show individual participant data, with bars representing the median values.

Please cite this article in press as: Dodd et al., Lymphocyte alterations and elevated complement signaling are key features of refractory myasthenia gravis, Med (2025), https://doi.org/10.1016/j.medj.2025.100987

CellPress
OPEN ACCESS

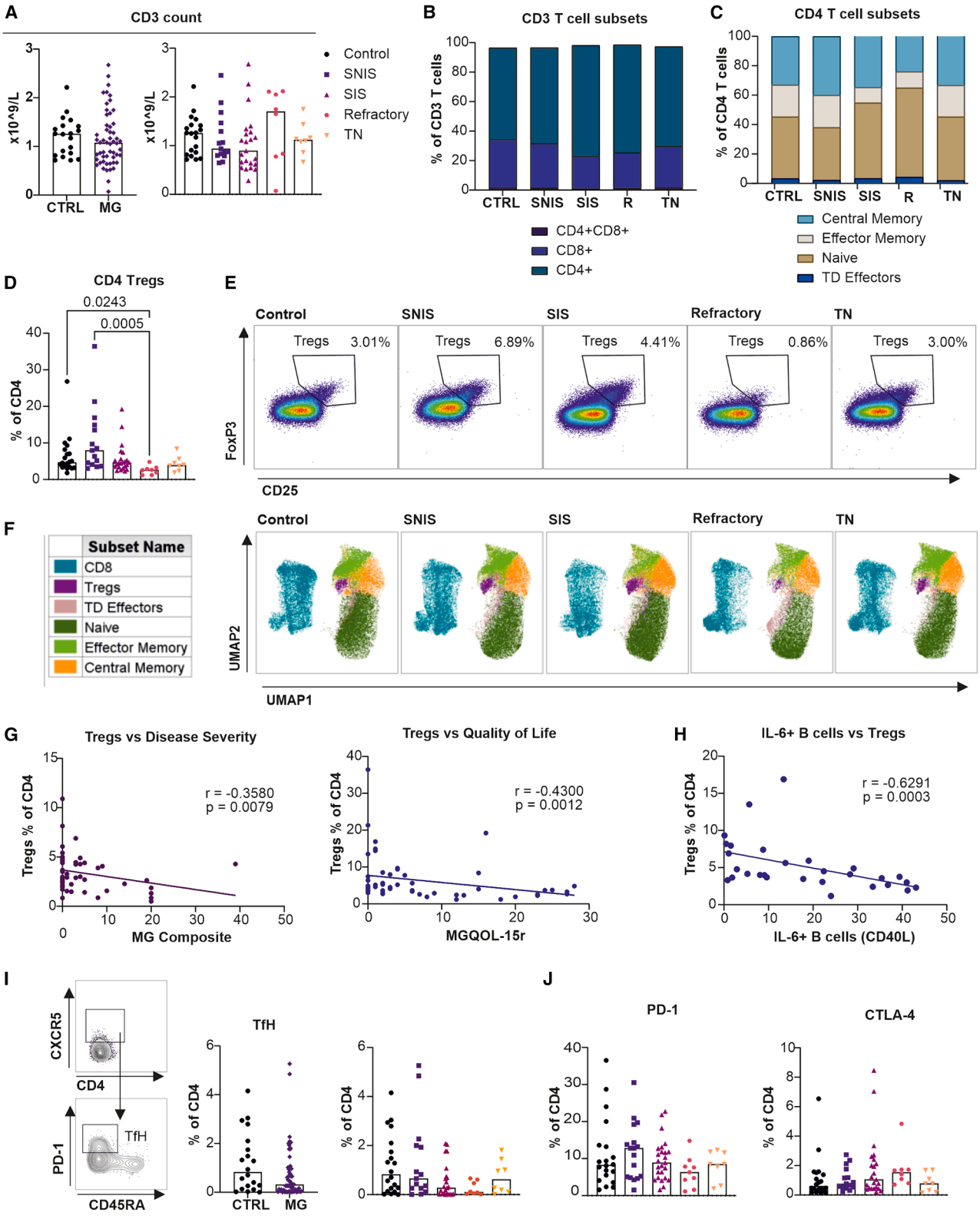

Figure 3. T cell alterations in patients with AChR-MG

(A) CD3 count, gated on live lymphocytes in PBMCs, in control ($n = 20$) compared to MG ($n = 54$) and between control ($n = 20$), SNIS ($n = 15$), SIS ($n = 23$), refractory ($n = 8$), and TN ($n = 8$) subgroups.

(legend continued on next page)

Please cite this article in press as: Dodd et al., Lymphocyte alterations and elevated complement signaling are key features of refractory myasthenia gravis, Med (2025), https://doi.org/10.1016/j.medj.2025.100987

CD35, and CD55 to see if this impacted cytokine production in a subset of samples. There was significantly reduced production of TNF-α from CD4 T cells upon stimulation in the context of CD55 inhibition (Figure 5G); no other significant differences were seen in the production of IL-6, IL-10, IL-17, TNF-α, or interferon (IFN)-γ (Figures S5A and S5B).

Unsupervised cluster analysis reveals defining features of refractory disease

To determine whether a distinct immune signature characterizes refractory MG, we applied principal-component analysis (PCA) followed by unsupervised *k*-means clustering to our flow cytometry dataset. This approach identified six discrete immune clusters (Figure 6A). Notably, cluster 1 was enriched for refractory patients with MG and was distinguished by a set of 16 immune markers (Figure 6B). Specifically, this refractory-patient-enriched cluster exhibited increased frequencies of $CD27^+$ B cells, memory and unswitched B cells, naive T cells, and CTLA-4^+ T cells, along with elevated CD55 expression on T cells. Cluster 1 also showed reduced frequencies of Tregs, central and effector memory T cells, $CD80^+$ DCs, and both mature and Ki-67^+ B cells. The patient-level heatmap illustrates that these immune alterations are consistently observed across most individuals in cluster 1 (Figure 6C), whereas the remaining clusters display more heterogeneous immune profiles. These findings support the existence of a distinct immune phenotype associated with refractory MG.

Low baseline B cell frequency is associated with poor response to rituximab

Eight of the 10 refractory participants were followed up at 1, 7, and 13 months following B cell depletion with two infusions of 1 g rituximab (or biosimilar) intravenously, 2 weeks apart. Some of these participants were given additional doses of rituximab at the clinician's discretion; the timing of these doses and changes in participant disease severity, quality of life, and prednisolone dose can be seen in Figure 7A. No changes in AChR-ab titers were observed (Figure S6A). All participants showed successful B cell depletion, with some participants displaying partial repopulation by month 13 (Figures 7B and 7C). Notably, those who did not reduce their severity score by 50% or more (defined as non-responders; R2, R4, and R7) had baseline B cell frequencies under 3%, whereas responders had baseline frequencies above 3%. Non-responders also had longer disease duration (median of 15 years) compared to responders (1 year).

Of the remaining B lineage cells in circulation during depletion, a high proportion of these were found to be plasmablasts, alongside increased Blimp-1 expression (Figures 7D, 7E, and S6A). In agreement with previous findings,[45] the repopulating B cells (in months 7–13) were found to be transitional ($CD24^{++}CD38^{++}$) and mature ($CD24^+CD38^+$) B cells (Figures 7D–7F). Residual B cells following depletion expressed less BAFF-R, CD21, and CD35 but not CD27 (Figures S6A and S6B).

Treg frequencies increased following B cell depletion in both responders and non-responders (Figures 7G and 7H). There were no significant changes in CD4 or CD8 T cell frequencies, T cell phenotype, or expression of PD-1 or CD55 (Figures S6C–S6E). It is noteworthy to mention that the rituximab clinical non-responders had the highest expression of CD55 in CD8 T cells at all time points (before and after rituximab treatment), suggesting that there was ongoing complement-mediated pathology (Figure 7G). Levels of C3, C5, and clusterin were unaltered in response to rituximab (Figures S6F–S6G). In the myeloid compartment, there was no change to DC or monocyte frequencies, but there was a trend to increasing NK cell frequencies (Figure S6H).

DISCUSSION

In MG, a proportion of patients remain refractory to therapy, and biomarkers to predict disease course and thus guide treatment decisions are lacking. This study is the broadest immunophenotyping study in AChR-MG to date, exploring circulating immune profiles in those with differing treatment requirements against age- and gender-matched controls. The pre-specified cohorts elucidated differences between those not requiring immunosuppression to obtain disease remission (SNIS), those responding to standard immunosuppression (SIS), and those who have not responded (refractory). We have identified a number of immune alterations that characterize refractory disease.

Circulating B cell frequencies are known to reduce with immunosuppression or long-standing autoimmune disease,[12] a finding we replicate here. We also replicate others' findings of class-switched memory B cell expansion in AChR-MG[14,46] but show that this is most marked in refractory disease. We also identified that the expansion of memory B cells is in EOMG rather than LOMG, which may translate to differences in the response to B cell-targeted therapies.

Surprisingly, we observed no differences in circulating plasmablast frequencies. This may be because AChR-abs are thought to be mainly produced by long-lived plasma cells, which reside in the bone marrow or lymphoid tissue rather than in circulation.[44,47] Two other studies have reported elevated plasmablast/plasma cell frequency in AChR-MG,[12,13] though these studies used

(B and C) (B) Proportion of $CD4^+$, $CD8^+$, and $CD4^+CD8^+$ cells, within $CD3^+$ live lymphocytes (B), and naive, central and effector memory, and TD effector T cell frequency, gated on $CD4^+$ T cells (C), in control (*n* = 20), SNIS (*n* = 15), SIS (*n* = 23), refractory (*n* = 8), and TN (*n* = 8).
(D) $FoxP3^+CD25^+$ Treg frequency, gated on both $CD4^+$ and $CD8^+$ T cells, in control (*n* = 20), SNIS (*n* = 15), SIS (*n* = 23), refractory (*n* = 8), and TN (*n* = 8).
(E) Representative FACS plots for Tregs in control, SNIS, SIS, refractory, and TN cohorts.
(F) Uniform manifold approximation and projection (UMAP) plots demonstrating main T cell subsets in a representative selection of 5,000 $CD3^+$ live lymphocytes of control (*n* = 8), SNIS (*n* = 8), SIS (*n* = 8), refractory (*n* = 8), and TN (*n* = 8).
(G) Simple linear regression for CD4 Treg frequency against MG Compositive and MG QoL-15r score (*n* = 54).
(H) Simple linear regression for CD4 Treg frequency against IL-6^+ B cells when stimulated with CD40L (*n* = 29).
(I) FACS plot demonstrating gating of $CXCR5^+CD45RA^-PD\text{-}1^+$ Tfh cells, gated on $CD4^+$ T cells, and graphs showing $CXCR5^+CD45RA^-PD\text{-}1^+$ Tfh cell frequency count in control (*n* = 20) compared to MG (*n* = 54) and between SNIS (*n* = 15), SIS (*n* = 23), refractory (*n* = 8), and TN (*n* = 8) subgroups.
(J) PD-1^+ and CTLA-4^+ CD4 T cell frequencies in control (*n* = 20), SNIS (*n* = 15), SIS (*n* = 23), refractory (*n* = 8), and TN (*n* = 8).
Flow cytometry was performed on PBMCs. Graphs show individual participant data, with bars representing the median values.

Please cite this article in press as: Dodd et al., Lymphocyte alterations and elevated complement signaling are key features of refractory myasthenia gravis, Med (2025), https://doi.org/10.1016/j.medj.2025.100987

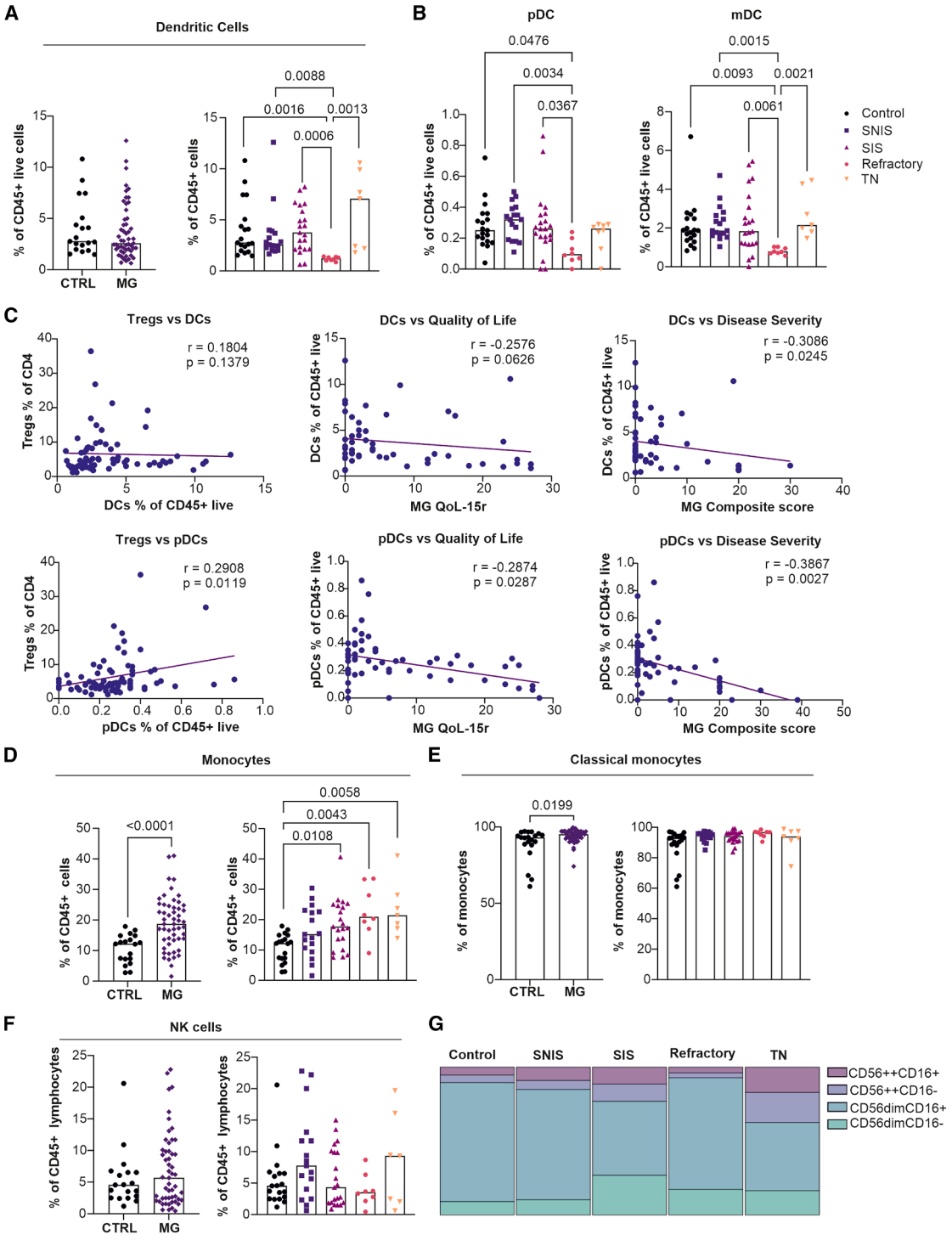

Figure 4. Myeloid cell alterations in patients with AChR-MG

(A) Frequencies of dendritic cells ($CD3^-CD19^-CD66b^-CD14^-HLA\text{-}DR^+$) in control ($n = 18$) compared to MG ($n = 48$) and in SNIS ($n = 17$), SIS ($n = 19$), refractory ($n = 6$), and TN ($n = 6$) subgroups.

(B) pDC and mDC frequency in control ($n = 18$), SNIS ($n = 17$), SIS ($n = 19$), refractory ($n = 6$), and TN ($n = 6$) subgroups.

(C) Simple linear regression for DCs and pDCs against Treg frequency ($n = 74$), quality of life ($n = 53$), and disease severity ($n = 53$).

(D) Frequencies of monocytes ($CD3^-CD19^-CD66b^-CD14^+HLA\text{-}DR^+CD64^+$) in control ($n = 18$) compared to MG ($n = 48$) and in SNIS ($n = 17$), SIS ($n = 19$), refractory ($n = 6$), and TN ($n = 6$) subgroups.

(E) Frequencies of classical monocytes in control ($n = 18$), compared to MG ($n = 48$) and in SNIS ($n = 17$), SIS ($n = 19$), refractory ($n = 6$), and TN ($n = 6$) subgroups.

(legend continued on next page)

Please cite this article in press as: Dodd et al., Lymphocyte alterations and elevated complement signaling are key features of refractory myasthenia gravis, Med (2025), https://doi.org/10.1016/j.medj.2025.100987

different markers than this study to define these cell types, and one did not include those on immunosuppression.

Although the pathogenic mechanism of MG is primarily the effects of AChR-ab at the neuromuscular junction, we found that there is a broad circulating pro-inflammatory phenotype, with B cells primed to produce pro-inflammatory cytokines IL-6 and TNF-α, in both EOMG and LOMG. IL-6 promotes plasma cell differentiation and autoantibody production, as well as inhibiting the formation of Tregs.[48] Conversely, Tregs are known to suppress pro-inflammatory B cell responses and promote regulatory B cell differentiation.[49] In line with this, we found that IL-6$^+$ B cell frequency correlated inversely with Treg frequency, which was significantly reduced in refractory disease (but not the SIS cohort), in keeping with a previous study.[50] Importantly, Treg frequencies negatively correlated with disease severity and quality-of-life scores, highlighting their potential as a biomarker for disease activity. Of interest, anti-IL-6 treatment has shown benefit for MG in a recently published randomized, controlled trial,[51] though Treg expansion strategies are also worthy of future study. Promoting immune tolerance confers a lower risk than widespread immunosuppression and can be done in a number of ways involving promoting regulatory innate immune cells,[52,53] possibly via vitamin D supplementation,[54] or adoptive transfer of Tregs, which has shown therapeutic benefit in the mouse model of MG.[55–57] Therapies promoting antigen-specific tolerance in AChR-MG have also been investigated in early studies.[58–63] However, there are multiple disease-associated AChR-Ab epitopes,[64] which suggests that these strategies would need to be tailored to the individual.

In addition, we identify a reduced frequency of DCs in refractory MG. A previous study showed decreased frequencies of pDCs, known to promote Treg differentiation,[65] in patients with MG compared to controls, with a reduced pDC:mDC ratio.[66] While a change in the pDC:mDC ratio was not observed within our patient cohort, we identified a reduction in circulating pDCs and mDCs in refractory disease. pDC frequency also correlated with Treg frequencies and inversely with disease severity and quality-of-life scores in patients with MG. This is in contrast to a recent study reporting higher frequencies of circulating pDCs and mDCs in patients with MG compared to controls.[19] Notably, that study contained an overwhelming majority of patients with mild disease (Myasthenia Gravis Foundation of America [MGFA] class I cases), with low numbers of those with severe disease.

In agreement with previous findings, our data show no differences in the frequency of naive, memory, or effector T cells in patients with MG compared to controls, in relation to treatment or severity.[67] However, in contrast to other studies reporting an expansion of Tfh cells, we observe a nominal reduction in patients compared to controls.[39] The prior study defined Tfh as CD3$^+$CD4$^+$CXCR5$^+$ cells, whereas we defined Tfh cells more robustly as CD3$^+$CD4$^+$CXCR5$^+$CD45RA$^-$PD-1$^+$ cells. This subset comprises a small population of the circulating T cells, and changes seen in the circulation may not correspond to those in lymphoid organs.

Expansion of monocytes was seen in patients with disease compared to controls, particularly in those with ongoing symptoms. Increased circulating classical monocyte frequencies may be promoting ongoing MHC class II antigen presentation but also have roles in inflammatory cytokine secretion and promotion of B cell survival.[68] Both monocytes and DCs displayed reduced CD86 expression in those stable on immunosuppression; for monocytes, this distinguished these patients from those who had not responded to immunosuppression (the refractory group). CD86 is the ligand for CD28 and CTLA-4 on T cells, and therefore, reduced expression may result in impaired T cell activation and regulatory function.[69]

A previous study examining NK cell frequencies in MG showed elevated frequencies in those in remission compared to those with disease exacerbation and controls.[70] In agreement with this study, we report a trend to higher frequencies of NK cells in the SNIS cohort, suggesting that they may play a protective role. Furthermore, other studies demonstrated a reduction in CD56$^+$CD16$^+$ NK cells, which correlated negatively with disease severity,[14] and an expansion of CD56dimCD16dim/- NK cells in patients with MG with a high disease burden, due to prior antibody-dependent cellular cytotoxicity (ADCC) activity.[71] However, we did not identify differences in NK cell subsets, perhaps due to differences in the therapies used by participants.

Circulating levels of total C3, C5, and the inhibitory molecule clusterin were elevated in the refractory cohort, correlating positively with disease severity and quality-of-life scores, positioning them as additional potential biomarkers of disease activity. Although other studies have reported varying results of complement levels, this might be attributed to a number of confounding factors, including laboratory methodology and participant characteristics.[22–25] Elevated serum C5a levels have previously been found to correlate with clinical severity.[25] Conversely, another study found a negative correlation between C3 and disease severity, proposed to be due to increased complement consumption.[22] We did not see a difference in complement proteins between EOMG and LOMG, in contrast to a previous study that reported lower C3 and C4 levels in EOMG.[23] Given the known heterogeneity of complement activation by AChR-Abs,[72] a prospective study of these complement markers prior to complement inhibitor therapies would allow assessment of their validity in predicting outcomes for targeted treatment.

We demonstrated a higher intensity of expression of complement receptors 1 (CD35) and 2 (CD21) on B cells, despite reduced frequencies of CD35$^+$ B cells in disease, which may result in lower regulatory effects.[30,31,73] Notably, the expression of CD55 and CD46 on T cells was also increased in MG, with the greatest difference on CD8 T cells in refractory disease. CD55 and CD46 function to inhibit the complement cascade, but ligation also has functional effects on T cells.[35] CD55 ligation on T cells reduces IFN-γ and IL-2 production and increases IL-10 production during antigen stimulation,[74] as well as having regulatory effects on CD8 T cell responses.[75] We found that inhibition

(F) Frequencies of NK cells in control (n = 18) compared to MG (n = 48) and in SNIS (n = 17), SIS (n = 19), refractory (n = 6), and TN (n = 6) subgroups.
(G) NK cell subtypes in control (n = 18), SNIS (n = 17), SIS (n = 19), refractory (n = 6), and TN (n = 6) subgroups.
Flow cytometry was performed on peripheral blood mononuclear cells (PBMCs). Graphs show individual participant data, with bars representing the median values.

Please cite this article in press as: Dodd et al., Lymphocyte alterations and elevated complement signaling are key features of refractory myasthenia gravis, Med (2025), https://doi.org/10.1016/j.medj.2025.100987

CellPress
OPEN ACCESS

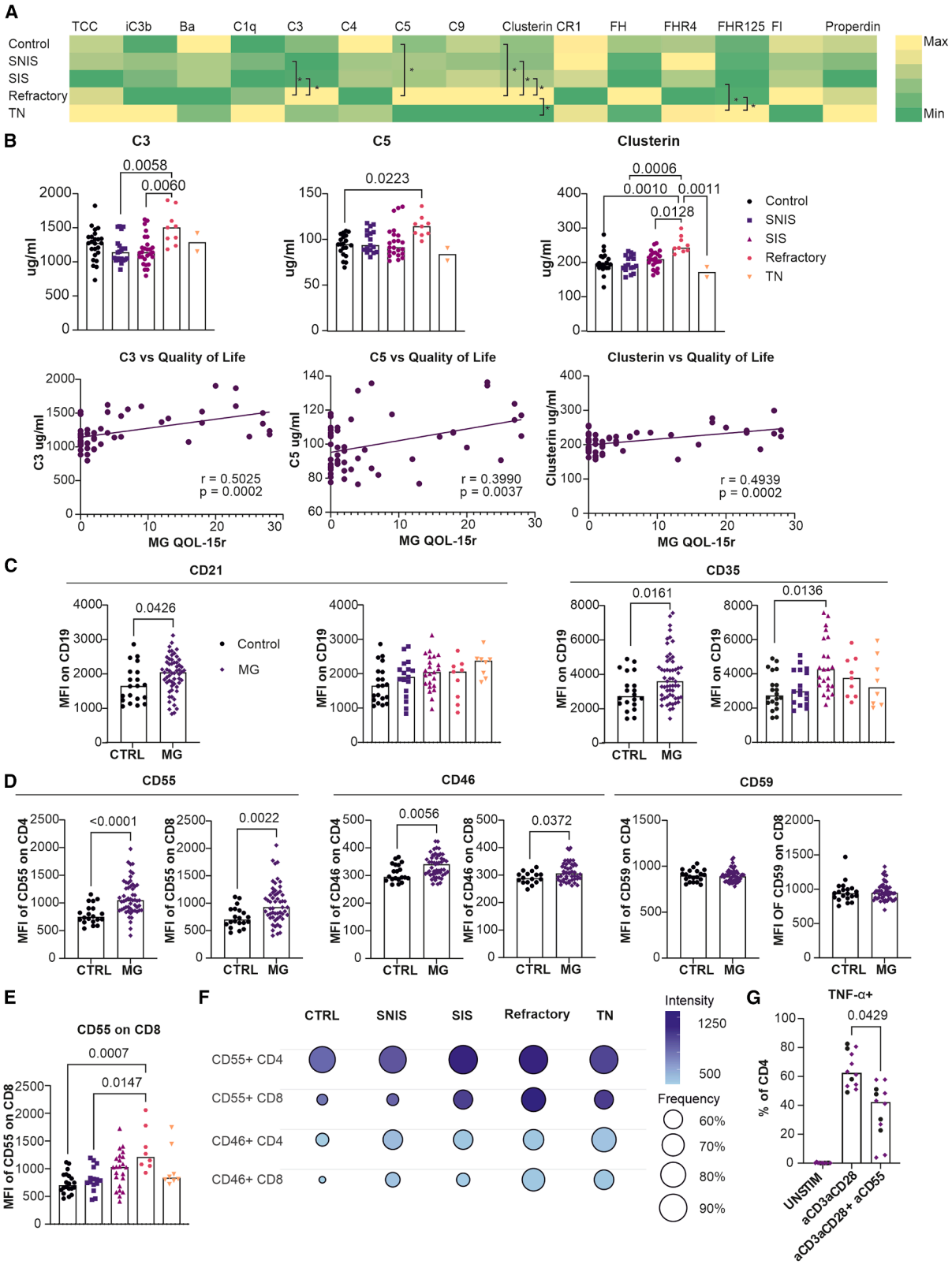

(legend on next page)

of CD55 in CD4 T cells reduced TNF-α production, further supporting its role in promoting pro-inflammatory cytokine release. Whereas CD46 binding initially results in IFN-γ production by CD4 T cells,[76] subsequent expansion of effector cells results in IL-2 accumulation, which then promotes Treg development.[77] This switch to IL-10 production does not occur in CD8 T cells, and therefore, the effects of CD46 on CD8 T cells are predominantly pro-inflammatory.[78] CD46 signaling has been shown to be dysregulated in several autoimmune conditions, with a lack of Treg differentiation upon CD46 co-stimulation.[77,79] We found a disconnect between elevated CD46 expression and Treg frequencies, suggesting that similar CD46 dysregulation may also occur in MG, warranting further mechanistic investigation.

Our interpretation of the immune changes relevant to refractory disease was corroborated by unsupervised clustering within the PCA. The refractory-rich cluster displayed a distinct immune signature, characterized by several alterations, including expanded memory B cells, enhanced CD55 expression in T cells, and a low frequency of Tregs. Of note, all three non-refractory members of this cluster had EOMG, which could have, in part, been relevant to some of the features seen.

Previous immune profiling relating to rituximab treatment for MG focuses on B cell repopulation rather than on baseline predictive markers. Early use of rituximab has previously been reported as an indication of good response,[80] a finding we replicated here. We found that the overall B cell frequency was <3% in all non-responders (those with a less than 50% reduction in disease severity score) and >3% in those with a ≥50% improvement. Although patient numbers are limited, this suggests that those early in disease will respond better than those with low B cell frequencies due to long-standing immunosuppression. Additionally, rituximab non-responders displayed the highest expression of CD55 in CD8 T cells, suggesting increased complement activity in these participants who may have benefited from complement-targeted therapy.

Following rituximab, the residual B cell population contained a high proportion of plasmablasts, most likely because B cells lose CD20 expression as they differentiate into plasmablasts and plasma cells. This highlights the disadvantage of targeting CD20 as opposed to CD19, CD38, or B cell maturation antigen (BCMA). An anti-CD19 monoclonal antibody has recently demonstrated efficacy,[81] and trial results for plasma cell-targeting therapies are eagerly anticipated.[82,83]

The remaining non-depleted B cells were of an altered phenotype, with low BAFF-R, CD21, and CD35 expression. BAFF-R expression has previously been shown to be reduced in CD19 cells following rituximab.[84] Importantly, Tregs are known to expand following rituximab,[50] a finding corroborated in this study.

Limitations of the study

The limitations of this study reflect those of many studies of MG. The wide heterogeneity of this rare disease makes it difficult to recruit to very specific cohorts while trying to extrapolate the findings to a wider population. Here, we attempted to limit this heterogeneity by only including those with AChR-ab-positive MG, with no thymoma or other autoimmune disease; however, other potential confounding factors such as differences in age, sex, ethnicity, socio-economic status, and other co-morbidities could have influenced the findings. Although power calculations were carried out to develop the protocol, recruitment fell short of planned numbers, and larger independent cohorts to validate these findings are required. The small number of refractory participants makes the interpretation of differences between the responders and non-responders challenging. Additionally, as a cohort study, it remains unknown whether the changes seen within the refractory cohort have evolved over time or are present at disease onset to predict outcome. Prospective recruitment of those with severe disease prior to initiation of immunotherapy is challenging; nevertheless, these findings may constitute the basis for future studies to validate these findings as predictive biomarkers.

Conclusion

In summary, significant alterations to the innate and adaptive immune systems are observed in AChR-MG, particularly in refractory disease. Frequency of memory B cells or Tregs or circulating C3, C5, or clusterin levels are potential prognostic markers that are worth further prospective evaluation. Our work suggests that future treatment strategies directed at plasma cells or at promoting immune tolerance mechanisms are likely to be beneficial in refractory disease.

RESOURCE AVAILABILITY

Lead contact

Further information and requests for resources and reagents should be directed to and will be fulfilled by the lead contact, Madhvi Menon (madhvi.menon@manchester.ac.uk).

Materials availability

This study did not generate new unique reagents.

Figure 5. Elevated circulating complement proteins and expression of complement receptors on lymphocytes in refractory MG

Complement proteins were measured by ELISA, and their receptor expression on PBMCs was analyzed by flow cytometry.

(A and B) (A) Heatmap demonstrating relative concentration of each complement protein analyzed (A) and frequencies of C3, C5, and clusterin (B) in control (n = 20), SNIS (n = 18), SIS (n = 23), refractory (n = 9), and TN (n = 2) subgroups, as well as correlation between C3, C5, clusterin, and quality of life (MG QoI-15r score) (n = 52) (B).

(C) Expression of CD21 and CD35 on B cells in control (n = 20) compared to MG (n = 56) and between control (n = 20), SNIS (n = 17), SIS (n = 22), refractory (n = 9), and TN (n = 8) subgroups.

(D) Graphs showing expression of CD55, CD46, and CD59 on CD4 and CD8 T cells in control (n = 20) compared to MG (n = 54).

(E) CD55 expression on CD8 T cells in control (n = 20), SNIS (n = 15), SIS (n = 23), refractory (n = 8), and TN (n = 8) subgroups.

(F) Bubble plot demonstrating frequency and intensity of expression of CD46 and CD55 on CD4 and CD8 T cells in control (n = 20), SNIS (n = 15), SIS (n = 23), refractory (n = 8), and TN (n = 8) subgroups.

(G) TNF-α^+ CD4 T cells in controls (n = 4) and MG (n = 8) when unstimulated, when stimulated with aCD3aCD28, and when stimulated with anti-CD55.

Graphs show individual participant data, with bars representing the median values.

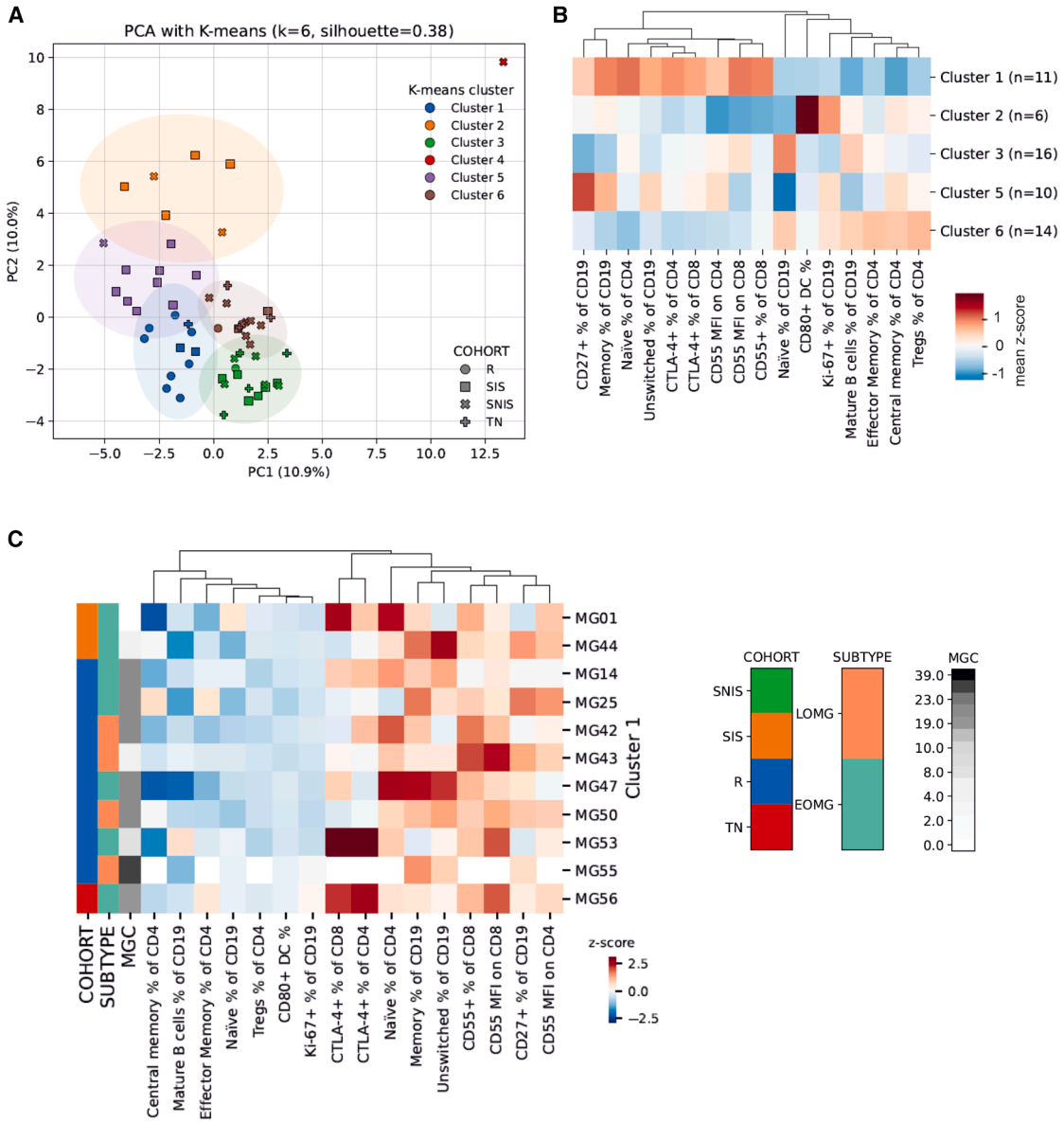

Figure 6. Distinct immune profile associated with refractory MG

(A) Two-dimensional principal-component analysis of *Z* scored flow markers. *k*-means on [PC1, PC2] identified six clusters. Points are colored by cluster and shaped by cohort; ellipses show 95% confidence contours in the PC space. PC1 and PC2 explain 10.9% and 10.0% of the variance, respectively.

(B) Heatmap of mean *Z* scores for the top 16 varying markers across the six *k*-means clusters. Colors indicate the mean *Z* scores (red = higher than the study-wide mean and blue = lower than the study-wide mean), centered at 0.

(C) Heatmap showing cluster 1 per-sample pattern across the top discriminating markers.

Data and code availability

- Data will be made available upon a written proposal and data transfer agreement.
- This study did not generate any original computer code.
- Any additional information required to reanalyze the data reported in this work paper is available from the lead contact upon request.

ACKNOWLEDGMENTS

We would like to acknowledge the study participants for their contribution; the University of Manchester Flow Cytometry Core Facility, Holly Sedgwick, Maana Layeghi, Halima Ali-Shuwa, Rinal Sahputra, Bethany Potts, and Sara Kirkham for assistance and technical expertise; and B. Paul Morgan and Tracy Hussell for intellectual input. This study was funded by the NorthCare Charity fund (CS2041), Myaware, and the Neuromuscular Study Group to K.D. and by the AMS Springboard Award (SBF006\1165) to M.M. M.M. is also the recipient of a UKRI Future Leaders Fellowship (MR/X03383X/1).

AUTHOR CONTRIBUTIONS

Conceptualization, K.C.D., J. Sussman, and M.M.; methodology, K.C.D., K.B., J.K.L.H., L.L., M.I.L., J. Spillane, S.V., W.M.Z., J. Sussman, P.W.W., and M.M.;

Please cite this article in press as: Dodd et al., Lymphocyte alterations and elevated complement signaling are key features of refractory myasthenia gravis, Med (2025), https://doi.org/10.1016/j.medj.2025.100987

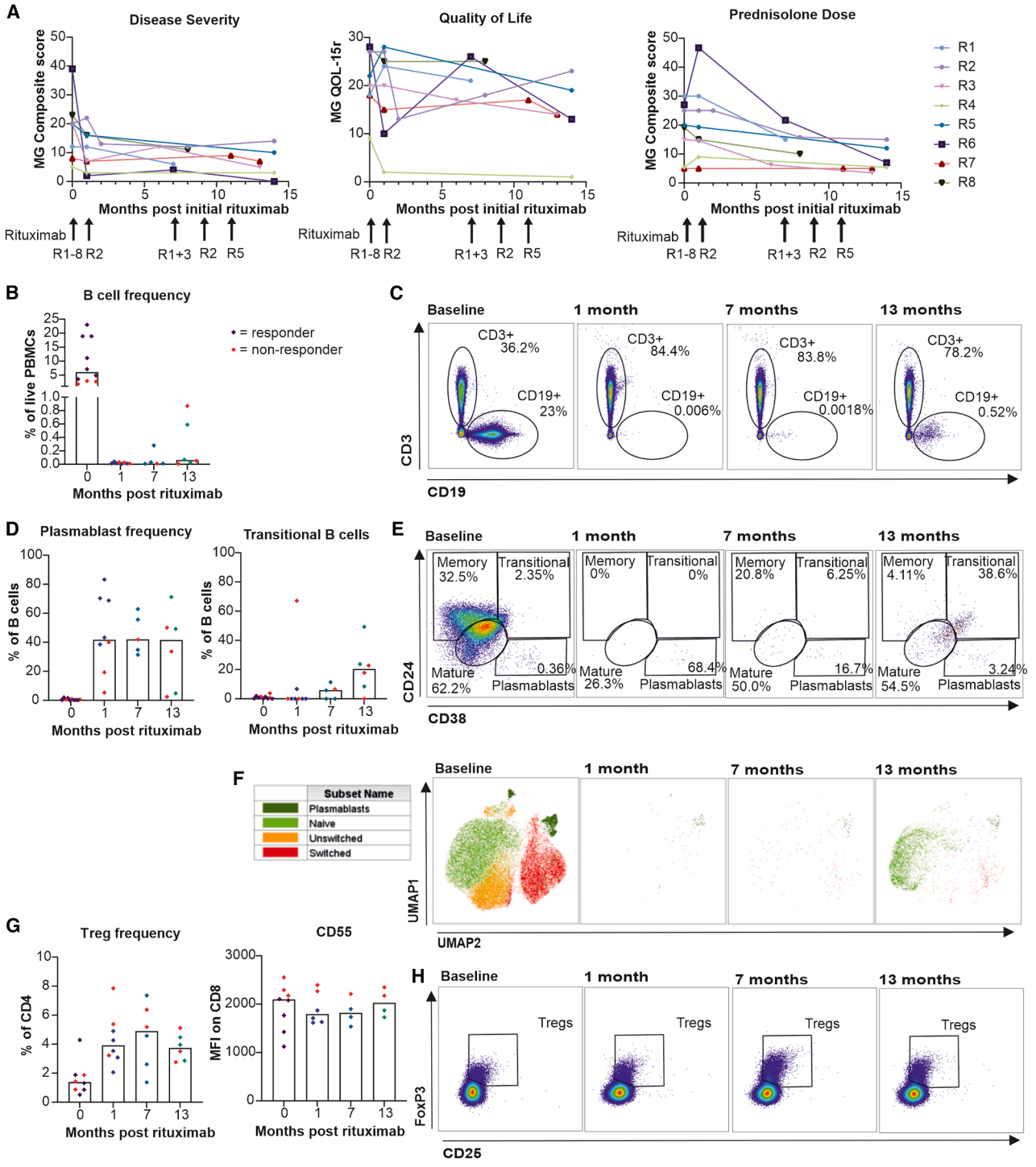

Figure 7. Immune alterations following B cell depletion therapy for refractory MG

(A) Disease severity, quality of life, and prednisolone dose changes following rituximab therapy. The timing of additional doses is indicated by arrows. Flow cytometry was performed on peripheral blood mononuclear cells (PBMCs) at baseline ($n = 10$) and at 1 ($n = 8$), 7 ($n = 5$), and 13 ($n = 6$) months post-rituximab in the refractory group.

(B) Changes in B cell frequency.

(C) Representative FACS plots showing changes in B and T cell frequency.

(D) Plasmablast and transitional B cell frequency.

(E) Representative FACS plots showing changes in B cell subsets.

(legend continued on next page)

investigation, K.C.D., K.B., J.K.L.H., L.L., M.I.L., J. Spillane, S.V., W.M.Z., J. Sussman, P.W.W., and M.M.; visualization and data analysis, K.C.D., L.L., P.W.W., and M.M.; funding acquisition, K.C.D. and J. Sussman; project administration, K.C.D.; supervision, J. Sussman and M.M.; writing – original draft, K.C.D. and M.M.; writing – review & editing, K.C.D., K.B., J.K.L.H., L.L., M.I.L., J. Spillane, S.V., W.M.Z., J. Sussman, P.W.W., and M.M. K.C.D., P.W.W., and L.L. performed the statistical analyses, with oversight from M.M. K.C.D. and P.W.W. performed the experiments. K.C.D., M.M., L.L., and P.W.W. had unrestricted access to all data. K.C.D. and M.M. prepared the first draft of the manuscript. All authors read, edited, and approved the final draft and take responsibility for the content.

DECLARATION OF INTERESTS

K.C.D. declares travel support and advisory fees from UCB. J.K.L.H. serves on paid advisory boards for Argenx and provides consultancy for Adivo Associates. M.I.L. has received speaker honoraria or travel grants from UCB Pharma and Horizon Therapeutics, consultancy fees from UCB Pharma, and serves on advisory boards for UCB Pharma, Argenx, and Horizon Therapeutics. J. Spillane has received speaker fees from Argenx, UCB, and J&J; travel support from Argenx and UCB; and has served on advisory boards for UCB, Argenx, and J&J. S.V. has received speaker honoraria or travel grants from UCB Pharma.

STAR★METHODS

Detailed methods are provided in the online version of this paper and include the following:

- KEY RESOURCES TABLE
- EXPERIMENTAL MODEL AND STUDY PARTICIPANT DETAILS
  - Ethics
  - Study design
- METHOD DETAILS
  - Sample processing
  - Flow cytometry
  - Cell stimulation
  - Complement immunoassays
- QUANTIFICATION AND STATISTICAL ANALYSIS
  - Sample size
  - Statistical analysis
  - Principal component analysis (PCA) and K-mean clustering in PCA space
- ADDITIONAL RESOURCES

SUPPLEMENTAL INFORMATION

Supplemental information can be found online at https://doi.org/10.1016/j.medj.2025.100987.

Received: April 23, 2025
Revised: June 10, 2025
Accepted: December 10, 2025

REFERENCES

1. Engel-Nitz, N.M., Boscoe, A., Wolbeck, R., Johnson, J., and Silvestri, N.J. (2018). Burden of illness in patients with treatment refractory myasthenia gravis. Muscle Nerve *58*, 99–105.
2. Harris, L., Graham, S., MacLachlan, S., Exuzides, A., and Jacob, S. (2019). Healthcare resource utilization by patients with treatment-refractory myasthenia gravis in England. J. Med. Econ. *22*, 691–697.
3. Lindstrom, J.M., Seybold, M.E., Lennon, V.A., Whittingham, S., and Duane, D.D. (1976). Antibody to acetylcholine receptor in myasthenia gravis. Prevalence, clinical correlates, and diagnostic value. Neurology *26*, 1054–1059.
4. Wolfe, G.I., Hanson, J.E., and Silvestri, N.J. (2024). Myasthenia gravis: The evolving therapeutic landscape. eNeurologicalSci *37*, 100541.
5. Luo, L., Zhu, X., Wen, C., Guo, Y., Yang, J., Wei, D., Yu, P., and Wan, M. (2024). Exploring the clinical significance of anti-acetylcholine receptor antibody titers, changes, and change rates in Myasthenia Gravis. Front. Neurol. *15*, 1506845.
6. Kojima, Y., Uzawa, A., Ozawa, Y., Yasuda, M., Onishi, Y., Akamine, H., Kawaguchi, N., Himuro, K., Noto, Y.-I., Mizuno, T., and Kuwabara, S. (2021). Rate of change in acetylcholine receptor antibody levels predicts myasthenia gravis outcome. J. Neurol. Neurosurg. Psychiatry *92*, 963–968.
7. Tian, W., Yu, H., Sun, Y., He, J., Wu, Q., Ma, C., Jiao, P., Huang, C., Li, D., and Tong, H. (2024). Thymoma negatively affects the neurological outcome of myasthenia gravis after thymectomy: a propensity score matching study. J. Cardiothorac. Surg. *19*, 37.
8. Wilcke, H., Glaubitz, S., Kück, F., Anten, C., Liebetanz, D., Schmidt, J., and Zschüntzsch, J. (2023). Female sex and overweight are associated with a lower quality of life in patients with myasthenia gravis: a single center cohort study. BMC Neurol. *23*, 366. https://doi.org/10.1186/s12883-023-03406-0.
9. Zhang, G.X., Xiao, B.G., Bakhiet, M., van der Meide, P., Wigzell, H., Link, H., and Olsson, T. (1996). Both CD4 and CD8 T cells are essential to induce experimental autoimmune myasthenia gravis. J. Exp. Med. *184*, 349–356. https://doi.org/10.1084/jem.184.2.349.
10. Thiruppathi, M., Rowin, J., Ganesh, B., Sheng, J.R., Prabhakar, B.S., and Meriggioli, M.N. (2012). Impaired regulatory function in circulating CD4 CD25highCD127low/− T cells in patients with myasthenia gravis. Clin. Immunol. *145*, 209–223. https://doi.org/10.1016/j.clim.2012.09.012.
11. Balandina, A., Lécart, S., Dartevelle, P., Saoudi, A., and Berrih-Aknin, S. (2005). Functional defect of regulatory CD4+ CD25+ T cells in the thymus of patients with autoimmune myasthenia gravis. Blood *105*, 735–741.
12. Kohler, S., Keil, T.O.P., Swierzy, M., Hoffmann, S., Schaffert, H., Ismail, M., Rückert, J.C., Alexander, T., Hiepe, F., Gross, C., et al. (2013). Disturbed B cell subpopulations and increased plasma cells in myasthenia gravis patients. J. Neuroimmunol. *264*, 114–119.
13. Zhang, Y., Jia, X., Xia, Y., Li, H., Chen, F., Zhu, J., Zhang, X., Zhang, Y., Wang, Y., Xu, Y., et al. (2018). Altered expression of transcription factors IRF4 and IRF8 in peripheral blood B cells is associated with clinical severity and circulating plasma cells frequency in patients with myasthenia gravis. Autoimmunity *51*, 126–134.
14. Fan, R., Que, W., Liu, Z., Zheng, W., Guo, X., Liu, L., and Xiao, F. (2022). Single-cell mapping reveals dysregulation of immune cell populations and VISTA+ monocytes in myasthenia gravis. Clin. Immunol. *245*, 109184.
15. Zhu, Z., You, W., Xie, Z., Wang, P., Liu, Z., Wang, C., and Bi, J. (2014). Mycophenolate mofetil improves neurological function and alters blood T-lymphocyte subsets in rats with experimental autoimmune encephalomyelitis. J. Int. Med. Res. *42*, 530–541.
16. Corey, A.L., Richman, D.P., Shuman, C.A., and Gomez, C.M. (1985). Use of monoclonal antiacetylcholine receptor antibodies to investigate the macrophage inflammation of acute experimental myasthenia gravis: refractoriness to a second episode of acute disease. Neurology *35*, 1455.

(F) UMAP plots displaying main B cell populations in all CD19$^+$ live lymphocytes (total = 195,944 cells).
(G) Changes in Treg frequency and CD55 expression in CD8 T cells.
(H) Representative FACS plots showing changes in Treg frequencies, gated on CD4$^+$ T cells.
All graphs show individual participant data, with bars representing the median values.

17. Utsugisawa, K., Nagane, Y., Suzuki, S., and Kondoh, R. (2007). Antigen-specific T-cell activation in hyperplastic thymus in myasthenia gravis. Muscle Nerve *36*, 100–103.

18. Nagane, Y., Utsugisawa, K., Obara, D., Yamagata, M., and Tohgi, H. (2003). Dendritic cells in hyperplastic thymuses from patients with myasthenia gravis. Muscle Nerve *27*, 582–589.

19. Song, Y., Xing, C., Lu, T., Liu, C., Wang, W., Wang, S., Feng, X., Bi, J., Wang, Q., and Lai, C. (2023). Aberrant dendritic cell subsets in patients with myasthenia gravis and related clinical features. Neuroimmunomodulation *30*, 69–80.

20. Dong, J., Duan, R.-S., and Zhang, P. (2024). Causal relationship between the immune phenotype of monocytes and myasthenia gravis: A Mendelian randomization study. Heliyon *10*, e26741.

21. Nakano, S., and Engel, A.G. (1993). Myasthenia gravis: Quantitative immunocytochemical analysis of inflammatory cells and detection of complement membrane attack complex at the end-plate in 30 patients. Neurology *43*, 1167. https://doi.org/10.1212/wnl.43.6.1167.

22. Romi, F., Kristoffersen, E.K., Aarli, J.A., and Gilhus, N.E. (2005). The role of complement in myasthenia gravis: serological evidence of complement consumption in vivo. J. Neuroimmunol. *158*, 191–194.

23. Liu, A., Lin, H., Liu, Y., Cao, X., Wang, X., and Li, Z. (2009). Correlation of C3 level with severity of generalized myasthenia gravis. Muscle Nerve *40*, 801–808.

24. Iacomino, N., Vanoli, F., Frangiamore, R., Ballardini, M., Scandiffio, L., Bortone, F., Andreetta, F., Baggi, F., Bernasconi, P., Antozzi, C., et al. (2022). Complement activation profile in myasthenia gravis patients: Perspectives for tailoring anti-complement therapy. Biomedicines *10*, 1360.

25. Aguirre, F., Manin, A., Fernandez, V.C., Justo, M.E., Leoni, J., Paz, M.L., and Villa, A.M. (2020). C3, C5a and anti-acetylcholine receptor antibody as severity biomarkers in myasthenia gravis. Ther. Adv. Neurol. Disord. *13*, 1756286420935697.

26. Tüzün, E., Scott, B.G., Goluszko, E., Higgs, S., and Christadoss, P. (2003). Genetic evidence for involvement of classical complement pathway in induction of experimental autoimmune myasthenia gravis. J. Immunol. *171*, 3847–3854.

27. Carroll, M.C. (2000). The role of complement in B cell activation and tolerance. Adv. Immunol. *74*, 61–88.

28. Dunkelberger, J.R., and Song, W.-C. (2010). Complement and its role in innate and adaptive immune responses. Cell Res. *20*, 34–50.

29. Yin, W., Allman, W., Ouyang, S., Li, Y., Li, J., Christadoss, P., and Yang, H. (2013). The increased expression of CD21 on AchR specified B cells in patients with myasthenia gravis. J. Neuroimmunol. *256*, 49–54.

30. Mácsik-Valent, B., Nagy, K., Fazekas, L., and Erdei, A. (2019). Complement Receptor Type 1 (CR1, CD35), the Inhibitor of BCR-Mediated Human B Cell Activation, Differentially Regulates TLR7, and TLR9 Induced Responses. Front. Immunol. *10*, 1493.

31. Kremlitzka, M., Mácsik-Valent, B., Polgár, A., Kiss, E., Poór, G., and Erdei, A. (2016). Complement Receptor Type 1 Suppresses Human B Cell Functions in SLE Patients. J. Immunol. Res. *2016*, 5758192.

32. Soltys, J., Halperin, J.A., and Xuebin, Q. (2012). DAF/CD55 and Protectin/CD59 modulate adaptive immunity and disease outcome in experimental autoimmune myasthenia gravis. J. Neuroimmunol. *244*, 63–69.

33. Kusner, L.L., Halperin, J.A., and Kaminski, H.J. (2013). Cell surface complement regulators moderate experimental myasthenia gravis pathology. Muscle Nerve *47*, 33–40.

34. Capasso, M., Durrant, L.G., Stacey, M., Gordon, S., Ramage, J., and Spendlove, I. (2006). Costimulation via CD55 on human CD4+ T cells mediated by CD97. J. Immunol. *177*, 1070–1077.

35. Longhi, M.P., Harris, C.L., Morgan, B.P., and Gallimore, A. (2006). Holding T cells in check–a new role for complement regulators? Trends Immunol. *27*, 102–108.

36. England, N.H.S. (2018). Clinical Commissioning Policy Statement: Rituximab bio-similar for the treatment of myasthenia gravis (adults).

37. Thiel, J., Schmidt, F.M., Lorenzetti, R., Troilo, A., Janowska, I., Nießen, L., Pfeiffer, S., Staniek, J., Benassini, B., Bott, M.-T., et al. (2024). Defects in B-lymphopoiesis and B-cell maturation underlie prolonged B-cell depletion in ANCA-associated vasculitis. Ann. Rheum. Dis. *83*, 1536–1548.

38. Luo, C., Li, Y., Liu, W., Feng, H., Wang, H., Huang, X., Qiu, L., and Ouyang, J. (2013). Expansion of circulating counterparts of follicular helper T cells in patients with myasthenia gravis. J. Neuroimmunol. *256*, 55–61.

39. Ashida, S., Ochi, H., Hamatani, M., Fujii, C., Kimura, K., Okada, Y., Hashi, Y., Kawamura, K., Ueno, H., Takahashi, R., et al. (2021). Immune Skew of Circulating Follicular Helper T Cells Associates With Myasthenia Gravis Severity. Neurol. Neuroimmunol. Neuroinflamm. *8*, e945. https://doi.org/10.1212/NXI.0000000000000945.

40. Makarious, D., Horwood, K., and Coward, J.I.G. (2017). Myasthenia gravis: An emerging toxicity of immune checkpoint inhibitors. Eur. J. Cancer *82*, 128–136.

41. Renton, A.E., Pliner, H.A., Provenzano, C., Evoli, A., Ricciardi, R., Nalls, M.A., Marangi, G., Abramzon, Y., Arepalli, S., Chong, S., et al. (2015). A genome-wide association study of myasthenia gravis. JAMA Neurol. *72*, 396–404.

42. Sun, L., Meng, Y., Xie, Y., Zhang, H., Zhang, Z., Wang, X., Jiang, B., Li, W., Li, Y., and Yang, Z. (2014). CTLA4 variants and haplotype contribute genetic susceptibility to myasthenia gravis in northern Chinese population. PLoS One *9*, e101986.

43. Wang, X.B., Pirskanen, R., Giscombe, R., and Lefvert, A.K. (2007). Two SNPs in the promoter region of the CTLA-4 gene affect binding of transcription factors and are associated with human myasthenia gravis. J. Intern. Med. *263*, 61–69. https://doi.org/10.1111/j.1365-2796.2007.01879.x.

44. Fichtner, M.L., Jiang, R., Bourke, A., Nowak, R.J., and O'Connor, K.C. (2020). Autoimmune Pathology in Myasthenia Gravis Disease Subtypes Is Governed by Divergent Mechanisms of Immunopathology. Front. Immunol. *11*, 776.

45. Dorcet, G., Migné, H., Biotti, D., Bost, C., Lerebours, F., Ciron, J., and Treiner, E. (2022). Early B cells repopulation in multiple sclerosis patients treated with rituximab is not predictive of a risk of relapse or clinical progression. J. Neurol. *269*, 5443–5453.

46. Hu, Y., Wang, J., Rao, J., Xu, X., Cheng, Y., Yan, L., Wu, Y., Wu, N., and Wu, X. (2020). Comparison of peripheral blood B cell subset ratios and B cell-related cytokine levels between ocular and generalized myasthenia gravis. Int. Immunopharmacol. *80*, 106130.

47. Hill, M.E., Shiono, H., Newsom-Davis, J., and Willcox, N. (2008). The myasthenia gravis thymus: a rare source of human autoantibody-secreting plasma cells for testing potential therapeutics. J. Neuroimmunol. *201*, 50–56.

48. Hirano, T. (2021). IL-6 in inflammation, autoimmunity and cancer. Int. Immunol. *33*, 127–148.

49. Wang, P., and Zheng, S.G. (2013). Regulatory T cells and B cells: implication on autoimmune diseases. Int. J. Clin. Exp. Pathol. *6*, 2668–2674.

50. Jing, S., Lu, J., Song, J., Luo, S., Zhou, L., Quan, C., Xi, J., and Zhao, C. (2019). Effect of low-dose rituximab treatment on T- and B-cell lymphocyte imbalance in refractory myasthenia gravis. J. Neuroimmunol. *332*, 216–223. https://doi.org/10.1016/j.jneuroim.2019.05.004.

51. Habib, A.A., Zhao, C., Aban, I., França, M.C., Jr., José, J.G., Zu Hörste, G.M., Klimiec-Moskal, E., Pulley, M.T., Tavolini, D., Krumova, P., et al. (2025). Safety and efficacy of satralizumab in patients with generalised myasthenia gravis (LUMINESCE): a randomised, double-blind, multicentre, placebo-controlled phase 3 trial. Lancet Neurol. *24*, 117–127.

52. Liu, J., and Cao, X. (2015). Regulatory dendritic cells in autoimmunity: A comprehensive review. J. Autoimmun. *63*, 1–12.

53. Sheng, J.R., Li, L., Ganesh, B.B., Vasu, C., Prabhakar, B.S., and Meriggioli, M.N. (2006). Suppression of experimental autoimmune myasthenia gravis by granulocyte-macrophage colony-stimulating factor is

associated with an expansion of FoxP3+ regulatory T cells. J. Immunol. *177*, 5296–5306.

54. Askmark, H., Haggård, L., Nygren, I., and Punga, A.R. (2012). Vitamin D deficiency in patients with myasthenia gravis and improvement of fatigue after supplementation of vitamin D3: a pilot study. Eur. J. Neurol. *19*, 1554–1560.

55. Danikowski, K.M., Jayaraman, S., and Prabhakar, B.S. (2017). Regulatory T cells in multiple sclerosis and myasthenia gravis. J. Neuroinflammation *14*, 117. https://doi.org/10.1186/s12974-017-0892-8.

56. Duffy, S.S., Keating, B.A., and Moalem-Taylor, G. (2019). Adoptive transfer of regulatory T cells as a promising immunotherapy for the treatment of multiple sclerosis. Front. Neurosci. *13*, 1107. https://doi.org/10.3389/fnins.2019.01107.

57. Himmel, M.E., Yao, Y., Orban, P.C., Steiner, T.S., and Levings, M.K. (2012). Regulatory T-cell therapy for inflammatory bowel disease: more questions than answers. Immunology *136*, 115–122.

58. Benne, N., Ter Braake, D., Stoppelenburg, A.J., and Broere, F. (2022). Nanoparticles for Inducing Antigen-Specific T Cell Tolerance in Autoimmune Diseases. Front. Immunol. *13*, 864403.

59. Keijzer, C., van der Zee, R., van Eden, W., and Broere, F. (2013). Treg inducing adjuvants for therapeutic vaccination against chronic inflammatory diseases. Front. Immunol. *4*, 245.

60. Serra, P., and Santamaria, P. (2020). Peptide-MHC-Based Nanomedicines for the Treatment of Autoimmunity: Engineering, Mechanisms, and Diseases. Front. Immunol. *11*, 621774.

61. Almenara-Fuentes, L., Rodriguez-Fernandez, S., Rosell-Mases, E., Kachler, K., You, A., Salvado, M., Andreev, D., Steffen, U., Bang, H., Bozec, A., et al. (2023). A new platform for autoimmune diseases. Inducing tolerance with liposomes encapsulating autoantigens. Nanomedicine *48*, 102635.

62. Curavac (2019). Safety, Tolerability and Immunogenic Response of CV-MG01 in Patients With Myasthenia Gravis. https://www.clinicaltrials.gov/study/NCT02609022?cond=Myasthenia%20Gravis&page=7&rank=64.

63. Ter Braake, D., Benne, N., Lau, C.Y.J., Mastrobattista, E., and Broere, F. (2021). Retinoic acid-containing liposomes for the induction of antigen-specific regulatory T cells as a treatment for autoimmune diseases. Pharmaceutics *13*, 1949.

64. Protti, M.P., Manfredi, A.A., Straub, C., Wu, X.D., Howard, J.F., Jr., and Conti-Tronconi, B.M. (1990). Use of synthetic peptides to establish anti-human acetylcholine receptor CD4+ cell lines from myasthenia gravis patients. J. Immunol. *144*, 1711–1720.

65. Ngo, C., Garrec, C., Tomasello, E., and Dalod, M. (2024). The role of plasmacytoid dendritic cells (pDCs) in immunity during viral infections and beyond. Cell. Mol. Immunol. *21*, 1008–1035.

66. Chen, P., Li, Y., Huang, H., Li, Y., Huang, X., Chen, Z., Liu, X., Qiu, L., Ou, C., Huang, Z., et al. (2019). Imbalance of the two main circulating dendritic cell subsets in patients with myasthenia gravis. Clin. Immunol. *205*, 130–137.

67. Melms, A., Malcherek, G., Gern, U., Sommer, N., Weissert, R., Wiethölter, H., and Bühring, H.J. (1993). Thymectomy and azathioprine have no effect on the phenotype of CD4 T lymphocyte subsets in myasthenia gravis. J. Neurol. Neurosurg. Psychiatry *56*, 46–51.

68. Mueller, C.G., Boix, C., Kwan, W.-H., Daussy, C., Fournier, E., Fridman, W.H., and Molina, T.J. (2007). Critical role of monocytes to support normal B cell and diffuse large B cell lymphoma survival and proliferation. J. Leukoc. Biol. *82*, 567–575.

69. Zheng, Y., Manzotti, C.N., Liu, M., Burke, F., Mead, K.I., and Sansom, D.M. (2004). CD86 and CD80 differentially modulate the suppressive function of human regulatory T cells. J. Immunol. *172*, 2778–2784.

70. Lai, X.-Y., Gui, M.-C., Lin, J., Li, Y., Luo, X., Li, L.-X., and Bu, B.-T. (2017). Peripheral NK and B regulatory cell frequencies are altered with symptomatic exacerbation in generalized myasthenia gravis patients. Neuroimmunol. Neuroinflammation *4*, 179–187.

71. Yandamuri, S.S., Filipek, B., Lele, N., Cohen, I., Bennett, J.L., Nowak, R.J., Sotirchos, E.S., Longbrake, E.E., Mace, E.M., and O'Connor, K.C. (2024). A Noncanonical CD56dimCD16dim/- NK Cell Subset Indicative of Prior Cytotoxic Activity Is Elevated in Patients with Autoantibody-Mediated Neurologic Diseases. J. Immunol. *212*, 785–800. https://doi.org/10.4049/jimmunol.2300015.

72. Obaid, A.H., Zografou, C., Vadysirisack, D.D., Munro-Sheldon, B., Fichtner, M.L., Roy, B., Philbrick, W.M., Bennett, J.L., Nowak, R.J., and O'Connor, K.C. (2022). Heterogeneity of acetylcholine receptor autoantibody–mediated complement activity in patients with myasthenia gravis. Neurol. Neuroimmunol. Neuroinflamm. *9*, e1169.

73. Kremlitzka, M., Polgár, A., Fülöp, L., Kiss, E., Poór, G., and Erdei, A. (2013). Complement receptor type 1 (CR1, CD35) is a potent inhibitor of B-cell functions in rheumatoid arthritis patients. Int. Immunol. *25*, 25–33.

74. Liu, J., Miwa, T., Hilliard, B., Chen, Y., Lambris, J.D., Wells, A.D., and Song, W.-C. (2005). The complement inhibitory protein DAF (CD55) suppresses T cell immunity in vivo. J. Exp. Med. *201*, 567–577.

75. Fang, C., Miwa, T., Shen, H., and Song, W.-C. (2007). Complement-dependent enhancement of CD8+ T cell immunity to lymphocytic choriomeningitis virus infection in decay-accelerating factor-deficient mice. J. Immunol. *179*, 3178–3186.

76. Sánchez, A., Feito, M.J., and Rojo, J.M. (2004). CD46-mediated costimulation induces a Th1-biased response and enhances early TCR/CD3 signaling in human CD4+ T lymphocytes. Eur. J. Immunol. *34*, 2439–2448.

77. Cardone, J., Le Friec, G., Vantourout, P., Roberts, A., Fuchs, A., Jackson, I., Suddason, T., Lord, G., Atkinson, J.P., Cope, A., et al. (2010). Complement regulator CD46 temporally regulates cytokine production by conventional and unconventional T cells. Nat. Immunol. *11*, 862–871.

78. Hansen, A.S., Slater, J., Biltoft, M., Bundgaard, B.B., Møller, B.K., and Höllsberg, P. (2018). CD46 is a potent co-stimulatory receptor for expansion of human IFN-γ-producing CD8 + T cells. Immunol. Lett. *200*, 26–32.

79. Astier, A.L., Meiffren, G., Freeman, S., and Hafler, D.A. (2006). Alterations in CD46-mediated Tr1 regulatory T cells in patients with multiple sclerosis. J. Clin. Investig. *116*, 3252–3257.

80. Brauner, S., Eriksson-Dufva, A., Hietala, M.A., Frisell, T., Press, R., and Piehl, F. (2020). Comparison between rituximab treatment for new-onset generalized myasthenia gravis and refractory generalized myasthenia gravis. JAMA Neurol. *77*, 974–981.

81. Nowak, R.J., Benatar, M., Ciafaloni, E., Howard, J.F., Jr., Leite, M.I., Utsugisawa, K., Vissing, J., Rojavin, M., Li, Q., Tang, F., et al. (2025). A phase 3 trial of inebilizumab in generalized myasthenia gravis. N. Engl. J. Med. *392*, 2309–2320.

82. Chang, T. (2024). Safety and Efficacy of CD19-BCMA Targeted CAR-T Therapy for Refractory Generalized Myasthenia Gravis. https://www.clinicaltrials.gov/study/NCT06371040?cond=Myasthenia%20Gravis&page=1&rank=9.

83. Takeda (2023). A Study of TAK-079 in People With Generalized Myasthenia Gravis. https://www.clinicaltrials.gov/study/NCT04159805?cond=Myasthenia%20Gravis&page=5&rank=49.

84. Becerra, E., Scully, M.A., Leandro, M.J., Heelas, E.O., Westwood, J.-P., De La Torre, I., and Cambridge, G. (2015). Effect of rituximab on B cell phenotype and serum B cell-activating factor levels in patients with thrombotic thrombocytopenic purpura. Clin. Exp. Immunol. *179*, 414–425.

85. Ozawa, Y., Uzawa, A., Yasuda, M., Kojima, Y., Oda, F., Himuro, K., Kawaguchi, N., and Kuwabara, S. (2021). Changes in serum complements and their regulators in generalized myasthenia gravis. Eur. J. Neurol. *28*, 314–322.

86. Lekova, E., Zelek, W.M., Gower, D., Spitzfaden, C., Osuch, I.H., John-Morris, E., Stach, L., Gormley, D., Sanderson, A., Bridges, A., et al.

(2022). Discovery of functionally distinct anti-C7 monoclonal antibodies and stratification of anti-nicotinic AChR positive Myasthenia Gravis patients. Front. Immunol. *13*, 968206.

87. Ozawa, Y., Uzawa, A., Onishi, Y., Yasuda, M., Kojima, Y., and Kuwabara, S. (2023). Activation of the classical complement pathway in myasthenia gravis with acetylcholine receptor antibodies. Muscle Nerve *68*, 798–804.

88. Nastuk, W.L., Plescia, O.J., and Osserman, K.E. (1960). Changes in Serum Complement Activity in Patients with Myasthenia Gravis. Proc. Soc. Exp. Biol. Med. *105*, 177–184.

Please cite this article in press as: Dodd et al., Lymphocyte alterations and elevated complement signaling are key features of refractory myasthenia gravis, Med (2025), https://doi.org/10.1016/j.medj.2025.100987

STAR★METHODS

KEY RESOURCES TABLE

REAGENT or RESOURCE	SOURCE	IDENTIFIER
Antibodies		
AF488, Blimp-1, clone 646702	R&D Systems	cat#IC36081G; RRID: AB_11129439
AF700, CD38, clone HIT2	Biolegend	cat#303524; RRID: AB_2072781
AF700, CD4, clone SK3	Biolegend	cat#344622; RRID: AB_2563150
AF700, CXCR5, clone J252D4	Biolegend	cat#356916; RRID: AB_2562290
AF700, IL-17A, clone BL168	Biolegend	cat#512318; RRID: AB_2124868
AF700, Ki67, clone Ki-67	Biolegend	cat#350530; RRID: AB_2564040
APC, CD123, clone 6H6	Biolegend	cat#306012; RRID: AB_439779
APC, CD21, clone Bu32	Biolegend	cat#354906; RRID: AB_2561454
APC, CD3, clone BW/264/56	Miltenyi	cat#130-113-125; RRID: AB_2725953
APC, CD59, clone p282	Biolegend	cat#304712; RRID: AB_2819930
APC, IL-10, clone JES3-19F1	Biolegend	cat#506807; RRID: AB_315457
APC/Fire 750, CD24, clone ML5	Biolegend	cat#311140; RRID: AB_2750463
APC/Fire 750, CD56, clone 5.1H11	Biolegend	cat#362554; RRID: AB_2572105
BV650, CD19, clone HIB19	Biolegend	cat#302238; RRID: AB_2562097
BV421, CCR7 (CD197), clone G043H7	Biolegend	cat#353208; RRID: AB_11203894
BV421, CD66b, clone 6/40c	Biolegend	cat#392915; RRID: AB_2888722
BV421, IgG, clone M1310G05	Biolegend	cat#410704; RRID: AB_2565626
BV510, CD279 (PD-1), clone EH12.2H7	Biolegend	cat#329932; RRID: AB_2562256
BV510, CD45, clone HI30	Biolegend	cat#304036; RRID: AB_2561940
BV510, IgM, clone MHM-88	Biolegend	cat#314522; RRID: AB_2562916
BV605, CD16, clone 3G8	Biolegend	cat#302040; RRID: AB_2562990
BV605, CD3, clone OKT3	Biolegend	cat#317322; RRID: AB_2561911
BV605, CD45RA, clone HI100	Biolegend	cat#304134; RRID: AB_2563814
BV605, IgD, clone IA6-2	Biolegend	cat#348232; RRID: AB_2563337
BV650, CD19, clone HIB19	Biolegend	cat#302238; RRID: AB_2562097
BV650, CD3, clone UCHT1	Biolegend	cat#300468; RRID:AB_2629574
BV711, CD274 (PD-L1), clone 29E.2A3	Biolegend	cat#329722; RRID: AB_2565764
BV711, CD86, clone IT2.2	Biolegend	cat#305440; RRID: AB_2565835
BV711, CD19, clone HIB19	Biolegend	cat#302246; RRID: AB_2562065
BV711, CD25, clone BC96	Biolegend	cat#302636; RRID: AB_2562910
BV711, CD274 (PD-L1), clone 29E.2A3	Biolegend	cat#329722; RRID: AB_2565764
BV711, IFN-G, clone 4S:B3	Biolegend	cat#502540; RRID: AB_2563506
BV785, CD11c, clone 3.9	Biolegend	cat#301644; RRID: AB_2565779
BV785, CD19, clone HIB19	Biolegend	cat#302240; RRID: AB_2563442
BV785, CD8, clone SK1	Biolegend	cat#344740; RRID: AB_2566202
PE, IL-6, clone MQ2-13A5	Biolegend	cat#501107; RRID: AB_315155
FITC, CD14, clone M5E2	Biolegend	cat#301804; RRID: AB_314186
FITC, CD35, clone E11	Biolegend	cat#333404; RRID: AB_2085022
FITC, FoxP3, clone 206D	Biolegend	cat#320106; RRID: AB_439752
PE/Cy7, TNF-α, clone MAb11	Biolegend	cat#502930; RRID: AB_2204079
PE Dazzle 594, CD27, clone M-T271	Biolegend	cat#356422; RRID: AB_2564101
PE Dazzle 594, CD303 (BDCA-2), clone 201A	Biolegend	cat#354226; RRID: AB_2629621

(*Continued on next page*)

Continued

REAGENT or RESOURCE	SOURCE	IDENTIFIER
PE Dazzle 594, CTLA-4 (CD152), clone L3D10	Biolegend	cat#349922; RRID: AB_2566198
PE Dazzle 594, IL-10, clone JES3-19F1	Biolegend	cat#506812; RRID: AB_2632783
PE, CD55 (DAF), clone JS11	Biolegend	cat#311308; RRID: AB_314865
PE, CD64, clone 10.1	Biolegend	cat#305008; RRID: AB_314492
PE, IL-6, clone MQ2-13A5	Biolegend	cat#501107; RRID: AB_315155
PE, CD35, clone E11	Biolegend	cat#333406; RRID: AB_2292231
PE/Cy7, BAFF-R, clone 11C1	Biolegend	cat#316920; RRID: AB_2565593
PE/Cy7, CD46 (MCP), clone TRA-2-10	Biolegend	cat#352408; RRID: AB_2564358
PE/Cy7, CD80, clone 2D10	Biolegend	cat#305218; RRID: AB_2076148
PE/Cy7, TNF-α, clone MAb11	Biolegend	cat#502930; RRID: AB_2204079
PerCP/Cy5.5, CD38, clone HIT-2	Biolegend	cat#303522; RRID: AB_893314
PerCP/Cy5.5, CD4, clone OKT4	Biolegend	cat#317428; RRID: AB_1186122
PerCP/Cy5.5, HLA-DR, clone L243	Biolegend	cat#307630; RRID: AB_893567
UV - 450, Live/dead, clone Zombie UV Fixable Viability Kit	Biolegend	cat#423107
Ba mAb D22/3	Hycult	cat#HM2379
iC3b mAb clone 9	Cardiff University	N/A
TCC mAb aE11	Hycult	cat#HM2167; RRID: AB_533189
C1q mAb 9H10	Cardiff University	N/A
C3 mAb 2898	Hycult	cat#HM2075; RRID: AB_533248
C4 Rabbit anti-C4	Cardiff University	N/A
C5 mAb 10B6	Cardiff University	N/A
C9 mAb B7	Cardiff University	N/A
Clusterin mAb 2D5	Cardiff University	N/A
sCR1 Rabbit anti-sCR1	Cardiff University	N/A
FH mAb OX24	Cardiff University	N/A
FHR4 mAb 4E9	Cardiff University	N/A
FHR125 mAb MBI125	Cardiff University	N/A
FI mAb 7B5	Cardiff University	N/A
Properdin mAb 9.3.4	Hycult	cat#HM2283
Ba mAb P21/15	Hycult	cat#HM2254; RRID: AB_1212111
iC3b mAb bH6	Hycult	cat#HM2168; RRID: AB_533007
TCC mAb E2 anti-C8-biotin	Cardiff University	N/A
C1q Rabbit anti-C1q	Cardiff University	N/A
C3 mAb clone 3	Hycult	cat#HM2257; RRID: AB_1953566
C4 Rabbit anti-C4	Cardiff University	N/A
C5 mAb 4G2	Cardiff University	N/A
C9 Rabbit anti-C9-biotin	Cardiff University	N/A
Clusterin mAb 4C7	Cardiff University	N/A
sCR1 mAb MBI35-HRP	Cardiff University	N/A
FH mAb 35H9-HRP	Cardiff University	N/A
FHR4 mAb clone 150-HRP	Cardiff University	N/A
FHR125 clone 35H9-HRP	Cardiff University	N/A
FI Rabbit anti-FI	Cardiff University	N/A
Properdin mAb clone 2.9	Hycult	cat#HM2282
anti-CD3, clone OKT3	Biolegend	cat#317326; RRID: AB_11150592
anti-CD28, clone CD28.6	eBioscience	cat#16-0288-85; RRID: AB_468925

(*Continued on next page*)

Please cite this article in press as: Dodd et al., Lymphocyte alterations and elevated complement signaling are key features of refractory myasthenia gravis, Med (2025), https://doi.org/10.1016/j.medj.2025.100987

Continued

REAGENT or RESOURCE	SOURCE	IDENTIFIER
anti-CD21, clone 1048	BD Bioscience	cat#552727; RRID: AB_394446
anti-CD55, rabbit polyclonal	AbCam	cat#ab231061
HRP-labelled anti-mouse	Jackson ImmunoResearch	cat#111-035-166
HRP-labelled anti-rabbit IgG	Jackson ImmunoResearch	cat#111-035-144; RRID: AB_2307391
Streptavidin-HRP	R&D Systems	cat#DY998
Biological samples		
Human blood	This paper	NHS Research Ethics Committee approval # 21/NW/0188
Chemicals, peptides, and recombinant proteins		
Ba	Comptech	cat#A113
iC3b	Comptech	cat#A115
TCC	Cardiff University	N/A
C1q	Cardiff University	N/A
C3	Cardiff University	N/A
C4	Comptech	cat#A108
C5	Cardiff University	N/A
C9	Cardiff University	N/A
Clusterin	Cardiff University	N/A
sCR1	Cardiff University	N/A
FH	Cardiff University	N/A
FHR4	Cardiff University	N/A
FHR125	Cardiff University	N/A
FI	Cardiff University	N/A
Properdin	Comptech	cat#A139
Human FcR Blocking Reagent	Miltenyi	cat#130-059-901; RRID: AB_2892112
FoxP3/transcription staining buffer set	Thermo Fisher	cat#00-5523-00
CD40L	R&D Systems	cat#aa 108-261
CpB-G	Cambridge Bioscience	cat#CpG ODN 10101
R848	Invivogen	cat#tlrl-r848
rCD35	Bio-Techne	cat#5748-CD
Brefeldin A	Biolegend	cat#420601
stimulation cocktail	Thermo Fisher	cat# 00-4970-93
OPD substrate	Sigma-Aldrich	cat#P9187
Software and algorithms		
FlowJo (version 10.9.0)	BD Biosciences	https://www.flowjo.com/
GraphPad Prism (version 10.0)	Graphpad	https://www.graphpad.com/features
R (version 4.5.2)	The R Foundation for Statistical Computing	https://www.r-project.org/
Python (version 3.13.5)	The Python Software Foundation	https://www.python.org/

EXPERIMENTAL MODEL AND STUDY PARTICIPANT DETAILS

Ethics

This study was approved by Health Research Authority and Health Care Research Wales and NHS Research Ethics Committee (21/NW/0188). Written informed consent was obtained for all enrolled participants.

Study design

Participants were recruited from the Northern Care Alliance NHS Foundation Trust, the Walton Center NHS Foundation Trust, Newcastle Hospitals NHS foundation Trust, Oxford, University College London NHS Foundation Trust, and Imperial NHS foundation

Please cite this article in press as: Dodd et al., Lymphocyte alterations and elevated complement signaling are key features of refractory myasthenia gravis, Med (2025), https://doi.org/10.1016/j.medj.2025.100987

Trust. Case Record Forms and clinical assessment were completed by the neurology clinical research fellow with each participant at baseline and follow-up. All participants were able to give valid consent and were aged 18 to 80. The following inclusion criteria applied to each cohort:

Stable Immunosuppressed participants have a diagnosis of AChR positive myasthenia gravis (can be ocular, bulbar or generalised), with MGFA Post-intervention Status MM or better with no clinical relapse for 2 years, on either azathioprine or MMF along with $\leq$5mg/day of prednisolone. They had no prednisolone dose increase or decrease in past 12 months, and no increase in azathioprine or MMF dose for 2 years (allowing for cessation for up to 1 month). Other medications for other indications were allowed. Stable Non-Immunosuppressed participants have a diagnosis of AChR positive myasthenia gravis (can be ocular, bulbar or generalised), with an MGFA Post-intervention Status MM or better on only low-dose cholinesterase inhibitors ($\leq$120 mg pyridostigmine/day on average) for over two years. Other medications for other indications were allowed. Refractory participants have a diagnosis of AChR positive myasthenia gravis (can be ocular, bulbar or generalised), and have been deemed eligible to be refractory to standard treatment and eligible for rituximab as per the NHS England criteria.[36] Treatment Naive participants have a diagnosis of AChR positive myasthenia gravis, diagnosed in previous 6 months, and have not yet taken any form of immunosuppression. Healthy Controls have no diagnosis of myasthenia gravis or other autoimmune condition that responds to standard immunosuppressive therapy (e.g., RA, inflammatory bowel disease).

Exclusion criteria for all cohorts included the presence of co-existing autoimmune conditions for which azathioprine or mycophenolate mofetil are treatments (e.g., inflammatory bowel disease, RA, neuromyotonia); currently undergoing treatment for solid organ or haematological malignancy, or previous thymoma; or a clinical frailty scale $\geq$6.

58 participants were included. Demographics and clinical features of the included participants can be seen in Table S1. Participants' information on sex, age, and race was physician-reported. Association of results with sex, age and race was not performed throughout due to limited sample size. Information on gender and socioeconomic status was not collected and therefore any associations could not be analyzed.

METHOD DETAILS

Sample processing

Whole blood was collected in two EDTA tubes and processed within 12 h of collection. Plasma was isolated from one tube via centrifugation of whole blood at 2000*g* for 10 min at room temperature. PBMCs were isolated from a separate tube using SepMate tubes (StemCell #85460), and Ficoll-Paque Plus (GE Healthcare # GE17-1440-03) via density gradient centrifugation (1200*g* for 10 min at room temp). Cells were washed twice in FACS buffer (PBS w/o Ca^{2+}/Mg^{2+}, 2%v/v FCS, 5 mM EDTA) prior to counting, using typtan blue and a countess II automated cell counter (Thermo Fisher Scientific). PBMCs were stored in FCS with 10% DMSO at -80°C for up to 2 weeks and then transferred to liquid nitrogen or -150°C storage.

Flow cytometry

Samples were thawed by warming at 37°C for 30 s then rapidly mixing with warmed complete media. Cells were washed in PBS then stained with Zombie UV (Biolegend, London UK) 1:500 for 15 min in PBS. Non-specific binding was blocked using Human FcR Blocking Reagent (Miltenyi, Bisley, UK) at 1:50 for 15 min. Extracellular antibodies were added at 1:50 for 30 min. Antibody information is provided in Table S2. Cells were then fixed and permeabilised using FOXP3/Transcription Factor Staining Buffer Set (Thermo Fisher, Altrincham, UK), washed in perm buffer and stained with intracellular markers at 1:100 overnight. Cells were acquired on the LSRFortessa (BD Biosciences, Swindon, UK) and data analyzed using FlowJo (v10.0; BD Biosciences). If under 50,000 lymphocytes were acquired, then results were excluded from analysis.

Cell stimulation

Thawed cells were stimulated with either CD40L (R&D Systems, Abbingdon, UK) 0.5 μg/mL CpG-B (Cambridge Bioscience, Cambridge, UK) 1 μM, or R848 (Resiquimod, InvivoGen Toulouse, France) 1 μg/mL for 48 h followed by 2 μL/mL of stimulation cocktail (Thermo Fisher) in the presence of Brefeldin A (Biolegend) in the last four hours, then washed and stained for flow cytometric analysis.

Thawed cells were also stimulated with R848 as above or placed into a plate which had been pre-coated for 1h at 37°C in PBS containing 1 μg/mL of each anti-CD3/anti-CD28 (clone OKT3, Biolegend (cat#317326)/clone CD28.6, eBioscience (cat#16-0288-85) respectively) in isolation or with anti-CD21 (clone 1048, BD Biosciences (cat#552727)) 10 μg/mL, rCD35 (Bio-Techne (cat#5748-CD)) 20 μg/mL or anti-CD55 (Rabbit poly-clonal, AbCam (cat#ab231061)) 25 μg/mL for 48 h followed by 2 μL/mL of stimulation cocktail (Thermo Fisher) in the presence of Brefeldin A (Biolegend) in the last four hours, then washed and stained for flow cytometric analysis.

Complement immunoassays

Fifteen complement analytes were selected based on previous research showing changes in serum levels of complement biomarkers in patients with MG and the accessibility of in house enzyme linked immunosorbent assays (ELISA),[85–88] The marker set was selected to interrogate the classical (C1q, C3, C4), alternative (Properdin, Ba, iC3b, FH, FHR125, FHR4, FI, sCR1), and terminal (C5, C9, clusterin, TCC (terminal complement complex)) pathways. Details of the antibodies, protein standards, and assay conditions can be

found in Table S3. Plasma samples stored at −80°C were thawed just before assaying, briefly vortexed, and then diluted in phosphate-buffered saline containing 0.1% Tween 20 (PBST, Sigma-Aldrich) and 0.2% bovine serum albumin (BSA) or non-fat milk (NFM; properdin assay only). Capture antibodies were fixed onto 96-well immunoplates (Thermo Fisher) overnight at 4°C, with concentrations ranging from 2 to 20 μg/mL in 50 μL/well of carbonate-bicarbonate buffer (pH 9.6). Wells were blocked with 2% BSA or NFM in PBST (100 μL/well) and incubated for 1 h at 37°C, washed once with PBST, and plasma samples or protein standards diluted in buffer (0.2% BSA or NFM PBST (50 μL/well) added in duplicate at a suitable dilution (Table S3). Plates were incubated for 1h at RT or 37°C, washed three times and detection antibodies added at appropriate concentration (1–5 μg/mL) in 50 μL/well 0.2% BSA or NFM in PBST for 1h at RT or 37°C. In assays where the detection antibody was not directly labeled, an HRP-labelled secondary antibody (anti-mouse or anti-rabbit IgG, as applicable, Jackson ImmunoResearch, West Grove, USA) or for biotinylated antibodies, Streptavidin-HRP (R&D Systems) was used. Finally, plates were washed and developed using O-phenylenediamine dihydrochloride (OPD) substrate (Sigma-Aldrich) for 3–15 min, followed by adding 50 μL/well 5% H_2SO_4 to quench the reaction. Absorbances were read at 492 nm using Infinite F50 microplate reader (Tecan, Reading, UK). Intra- and inter-assay coefficient of variation were below 10% for all assays.

QUANTIFICATION AND STATISTICAL ANALYSIS

Sample size

Sample size was calculated on previous unpublished data comparing CD19 count between those on effective immunosuppression and those not; for a power of 80% and a significant level of 5%, 23 participants were required in each group and we therefore attempted to recruit 24 to each cohort.

Statistical analysis

Statistical analysis was undertaken using GraphPad PRISM (version 10.0). All data underwent normality testing (Shapiro-Wilk test). Comparison between disease and control was with Student's *t* test (parametric data) or Mann-Whitney (non-parametric). Comparison between cohorts was with one-way ANOVA with Tukey multiple comparison test (parametric) or Kruskal-Wallis with Dunn's multiple comparison test (non-parametric). Results are presented as individual data points with medians. For correlation Pearson's correlation (for parametric) or Spearman's rank correlation coefficient test (for non-parametric data). In all cases, a p value of ≤ 0.05 was considered significant. Where no statistical difference is shown, there was no significant difference. Details of statistical tests and definitions of n can be found in each figure legend. The bubble plot in Figure 5 was created using R (version 4.5.2).

Principal component analysis (PCA) and K-mean clustering in PCA space

Flow cytometry markers were screened for missingness at the variable level (using Python version 3.13.5); any marker with >30% missing data was excluded (six markers removed: TNF-α^+ B cells with R848, 74%; TNF-α^+ B cells with CpG-B, 69%; IL-6^+ B cells with CpG-B, 69%; IL-6^+ B cells with R848, 67%; TNF-α^+ B cells with CD40L, 64%; IL-6^+ B cells with CD40L, 64%). Where the remaining analyses required complete data, remaining missing entries were then imputed using the per-marker median across samples, and all retained markers were standardised to z-scores (mean = 0, SD = 1).

Principal component analysis (PCA) was fitted to the z-scored matrix and the first two components (PC1, PC2) were used for visualisation. Unsupervised clustering was performed in the PC1–PC2 plane using K-means with a pre-specified number of clusters k; separation quality was summarised by the silhouette score. For each cluster, a confidence ellipse was drawn in PC space, centered at the cluster mean, oriented by the eigenvectors of the within-cluster covariance, and scaled to approximate a 95% contour.

For marker-level inference, a single target cluster from the K-means solution was compared with all other samples. For every marker, we computed Cohen's d (standardised mean difference with a pooled standard deviation) contrasting the target cluster against the remainder and additionally obtained two-sided Mann–Whitney U p-values. Markers were deemed different if they satisfied both criteria: $p < 0.05$ and $|d| \geq 0.5$. To summarise multivariate patterns, we plotted a heatmap of mean z-scores for the target cluster versus others (rows) across markers (columns); where helpful, marker columns were hierarchically ordered to group similar response profiles.

ADDITIONAL RESOURCES

This study was registered on clinicaltrials.gov ID: NHS001843.